

Review

Implementation of the Chick Chorioallantoic Membrane (CAM) Model in Radiation Biology and Experimental Radiation Oncology Research

Nicole Dünker ^{1,*}  and Verena Jendrossek ^{2,*} 

¹ Institute for Anatomy II, Department of Neuroanatomy, University of Duisburg-Essen, University Medicine Essen, 45122 Essen, Germany

² Institute of Cell Biology (Cancer Research), University of Duisburg-Essen, University Medicine Essen, 45122 Essen, Germany

* Correspondence: Nicole.Duenker@uk-essen.de (N.D.); Verena.Jendrossek@uk-essen.de or verena.jendrossej@uni-due.de (V.J.); Tel.: +49-0201-723-4299 (N.D.); +49-0201-723-3380 (V.J.)

Received: 2 September 2019; Accepted: 20 September 2019; Published: 7 October 2019



Abstract: Radiotherapy (RT) is part of standard cancer treatment. Innovations in treatment planning and increased precision in dose delivery have significantly improved the therapeutic gain of radiotherapy but are reaching their limits due to biologic constraints. Thus, a better understanding of the complex local and systemic responses to RT and of the biological mechanisms causing treatment success or failure is required if we aim to define novel targets for biological therapy optimization. Moreover, optimal treatment schedules and prognostic biomarkers have to be defined for assigning patients to the best treatment option. The complexity of the tumor environment and of the radiation response requires extensive *in vivo* experiments for the validation of such treatments. So far *in vivo* investigations have mostly been performed in time- and cost-intensive murine models. Here we propose the implementation of the chick chorioallantoic membrane (CAM) model as a fast, cost-efficient model for semi high-throughput preclinical *in vivo* screening of the modulation of the radiation effects by molecularly targeted drugs. This review provides a comprehensive overview on the application spectrum, advantages and limitations of the CAM assay and summarizes current knowledge of its applicability for cancer research with special focus on research in radiation biology and experimental radiation oncology.

Keywords: chorioallantoic membrane assay; CAM; radiation; radiotherapy; radioresistance; hypoxia; cancer; tumor; molecularly targeted drugs; tumor microenvironment

1. Introduction

About 50% of all cancer patients receive radiotherapy (RT) at some point during the course of their disease (World Health Organization, WHO) and good results in terms of long-term survival and tumor cure are achieved in a variety of tumors by multimodal combinations of surgery, RT, and chemotherapy [1]. Yet cure rates remain still unsatisfactory for common forms of cancer with high loco-regional failure-rates or frequent development of metastases. Though patient-specific clinical factors may explain some of these failures, it is commonly assumed that multiple biological factors adversely affect the response of tumor cells to treatment. Major biological limitations to successful RT comprise tumor-promoting mutations, unfavorable gene expression profiles, high intrinsic cancer cell radioresistance, a resistance-promoting microenvironment, hypoxia, heterogeneity in tumor and normal tissue radiation responses, phenotypic plasticity of cancer cells in adverse environments, tumor heterogeneity, as well as enrichment in radioresistant tumor stem cells [2]. Moreover, acute and late toxicity to normal tissues limit the radiation dose that can be safely applied to the tumor and decrease

the quality of life of cancer patients, whereas tolerable doses are often linked to suboptimal tumor control [3–7]. These limitations highlight the high medical need for innovations in RT practice.

Innovative strategies for improving treatment outcome therefore aim to selectively enhance toxicity to the tumor, reduce complications in normal tissues, or both. During recent years, the practice of RT has substantially benefited from technical improvements in treatment planning and increased accuracy of dose delivery (e.g., stereotactic RT or intensity-modulated radiation therapy (IMRT)), as well as by the development of particle therapy approaches [8]. Charged particles (mainly protons and carbon ions) have depth-dose distributions and linear energy transfer (LET) characteristics that allow the deposition of high and more effective radiation doses to deep-seated regions in a patient [8–11].

Safety and effectiveness of therapy with protons or other charged particles are currently evaluated in clinical studies in specialized centers for carefully selected tumor sites [12–14]. For example, the advantageous physical and radiobiological characteristics of carbon ions make carbon ion therapy an attractive approach for the treatment of hypoxic tumors with pronounced radioresistance, e.g., non-small cell lung cancer [15–17]. Nevertheless, further preclinical work is required to define the relative biological effectiveness (RBE) of particle beams of different energies in clinically relevant tumor entities *in vitro* and *in vivo*. Furthermore, the increased RBE of carbon ion beams compared to photon and proton beams with respect to the eradication of clonogenic tumor cells and the reduction in tumor burden may also increase the risk for acute and chronic adverse effects in tissues and organs with high intrinsic radiosensitivity such as the normal lung tissue [18–23]. It is thus also important to evaluate the RBE of protons, carbon ions, and heavy ions with respect to sensitivity of cells from normal tissues *in vitro* as well as the tolerance of highly radiosensitive normal tissues and organs to such treatments in preclinical models *in vivo* [19,24,25]. Taken together, despite success, improving cure-rates through technical and physical improvements in accurate dose delivery has some natural limits defined by the biological characteristics of the tumor or the infiltration of critical normal-tissue structures by malignant cells that cannot be spared, further underlining the need for further innovation in radiotherapy practice.

2. Biologic Optimization of Radiotherapy

Another important approach for improving cure rates focuses on the biologic optimization of RT by targeted modulation of biological processes that determine the radiation response of normal and tumor tissues. A few successful examples document promise of such approaches: RT plus androgen deprivation to treat locally advanced prostate cancer or RT plus cetuximab, an inhibitory antibody against the epidermal growth factor receptor (EGFR), to treat head and neck cancer patients not tolerating concurrent cisplatin chemotherapy (CT) [26–29] and more recently, immunotherapy [30,31]. However, other clinical trials combining chemoradiotherapy (CRT) with small molecule signal transduction inhibitors did not yet translate into clinical practice [29] or have even been negative due to low efficacy or complications [32–35]. Thus, further preclinical work is required to gain a better understanding of the complex local and systemic responses to RT and their modulation by application of targeted drugs, of intra- and inter-cellular signaling networks that control cell radiosensitivity and cell fate decisions, and of the mechanisms driving microenvironment-mediated resistance if we aim to design effective strategies for radiation response modulation [3,36,37].

Improvements in the outcome of patients with locally advanced tumors are currently expected from treatment protocols combining precision RT using highly conformal photon radiotherapy or particle therapy with molecularly targeted small molecules targeting for example signaling pathways in tumor cells or environmental factors promoting cancer (stem) cell radioresistance, genetic vulnerabilities, cancer driving mutations, or other malignant cancer traits [25,37–41]. Herein, the identification of specific differences in radiation response pathways and genetic vulnerabilities between cancer and normal cells will offer unique opportunities for cancer cell-specific modulation of the radiation response.

DNA double strand breaks (DSB) are the most crucial lesions induced by ionizing radiation. Cells resist the toxic effects of ionizing radiation by mounting an efficient DNA damage response

(DDR) [42] to regulate, adapt, and coordinate many vital cellular functions upon detection of DSBs, and to effectively repair radiation-induced lesions, particularly DSBs. Thus, compounds that suppress DDR or DSB repair have the potential for tumor radiosensitization, particularly when they affect tumor cells more than the surrounding normal tissue; vice-versa, compounds that selectively enhance DDR and DSB repair in normal cells may be used for normal tissue protection [3,43–48]. Currently, exciting potential for innovation arises from the identification of cancer cell-specific or context-dependent (e.g., severe hypoxia) deficiencies in DNA repair or genomic stability, that may be exploited for cancer cell-specific or tumor region-selective radiosensitization, respectively [45,49–55].

Of note, preclinical investigations revealed differences in the quality of DNA damage induced by irradiation with photons and charged heavy ions [56–62] and potentially even between photons and protons [11,63,64]. The enhanced requirement for specific DNA repair pathways, particularly homologous recombination repair (HRR), may have potential relevance for stratification of patients carrying mutations in DNA damage response or DNA repair pathways [63]. The assumed enhanced vulnerability of such cancer cells to proton or particle irradiation may open new avenues for optimization of particle therapy. However, extensive further preclinical work is required to further define the underlying mechanisms and to explore the potential of such differences for the design of rational and effective combinatorial approaches using proton therapy or therapy with other charged particles in combination with targeted DNA damage response modifiers. Successful individualization of RT quality and mechanism-based combinatorial strategies in the clinics will depend on the definition of reliable biomarkers or alternatively of gene-expression, miRNA-expression or protein-expression profiles predictive for individual tumor and normal tissue radiosensitivity; such profiles can be identified by systematic multiomics analysis of individual expression profiles in irradiated individual tumor and normal tissues of individual patients [39,40,65–68].

Another emerging concept for biology-based optimization of RT is based on the observation that the tumor stroma impacts cancer cell radiosensitivity at multiple levels and may thus provide attractive therapeutic targets. Herein, extracellular matrix (ECM) molecules, tumor microvessels, the vascular stem cell niche, accessory host cells (e.g., fibroblasts and cells of the innate and adaptive immune systems), and secreted factors constitute important determinants of the tumor response to RT, at least in preclinical investigations [69–75]. Although the first observations about a potential contribution of the host immune system to successful tumor eradication by the local application of ionizing radiation date more than 100 years ago (for review see: [76]), clinical observations about radiation-induced eradication of tumor lesions outside the radiation field (abscopal effects) remained rare [77]. The progress in immunotherapy and the seminal discoveries that radiotherapy can overcome immunosuppressive barriers in the tumor microenvironment, induce immunogenic alterations in tumor cells, and even elicit local and systemic T-cell-mediated antitumor immune responses expedited interest in exploiting the benefit of combining radiotherapy with immunotherapy [30,31,77–91]. This knowledge is now being increasingly used in the design of new treatment strategies, e.g., by combining RT with immunotherapy [84,92–94]. For example, first clinical studies revealed that lung cancer patients benefit from a treatment with inhibitors of the programmed cell death protein1 (PD1)/PD-1 ligand 1 (PDL1) immune checkpoint when given after RT or platinum-based CRT with improved progression-free survival and that this treatment had an acceptable safety profile [95,96]. However, a better understanding of the multifactorial mechanisms driving tumor immune escape, radiation-induced immune activation, and the reciprocal interactions between RT-induced and immunotherapy-induced immune changes is needed to optimally exploit RT-induced immune enhancement e.g., in combination with immune checkpoint inhibition, and to avoid the development of therapy resistance and excessive toxic side effects [97–104] and these investigations require *in vivo* models.

Finally, the microenvironment of solid human tumors is frequently characterized by reduced oxygen tensions including tumor types with pronounced radioresistance [105]. This so-called tumor hypoxia mostly coexists with a low tumor pH (tumor acidosis) further aggravating the hostile tumor environment [106]. Tumor hypoxia results from an imbalance between the pronounced oxygen

demand by rapidly growing and proliferating cancer cells and an insufficient oxygen supply that is limited by irregular blood flow, a chaotic and dysfunctional tumor microvasculature, and potentially a reduced oxygen transport capacity and limited oxygen saturation in cancer patients [107–109]. Tumor hypoxia has prognostic relevance and is associated with poor patient outcome independent of their respective treatment [110]. However, except for heavy particle therapy with carbon ions tumor hypoxia is particularly relevant in radiation oncology as already highlighted more than 50 years ago [111] and confirmed by multiple reports about the prognostic value of pre-therapeutic tumor hypoxia to patient outcome upon RT [112–114]. Tumor hypoxia constitutes a major biological obstacle to successful RT for multiple reasons: On the one hand, the cytotoxic efficacy of RT relies on the formation of reactive oxygen species (ROS) and thus on local availability of molecular oxygen (O_2) during treatment delivery. An acute decrease in O_2 levels will thus result in reduced DNA damage and thus confer direct resistance to RT-induced cell killing [115–117]. These observations led to the concept of using of hyperbaric oxygenation [118], oxygen mimics, hypoxia-activated pro-drugs and hypoxia active drugs for radiosensitization as recently reviewed elsewhere [114]. Interestingly, pharmacologic approaches reducing oxygen consumption by metabolic inhibition turned out to be much more efficient in increasing oxygen availability in hypoxic tumors than approaches to increase oxygen delivery [119–125]. Furthermore, O_2 deprivation restrains proliferation and activates drug-resistance genes as well as survival pathways that decrease therapy-induced cell death and promote treatment failure [126–129]; these observations make components of hypoxia-activated survival pathways promising therapeutic targets to overcome RT resistance in acute hypoxia [129,130]. However, oxygen availability in hypoxic tumor regions is not only highly heterogeneous ranging from mild ($<5\% O_2$) to severe hypoxia ($<0.5\% O_2$) or even anoxia ($<0.01\% O_2$) but also highly dynamic with respect to its duration and schedule (acute, transient, chronic, or intermittent) and also fluctuates regionally presumably as a result of the instability and chaotic organization of the tumor vasculature [109,131–134]. Substantial fractions of human solid tumors are thus exposed to dynamic cycles of hypoxia and intermittent re-oxygenation that have been demonstrated to drive adaptive responses and phenotypic heterogeneity as well as malignant progression by increasing genomic instability, generation and maintenance of cancer stem cells, cancer cell metastasis, and the clonal evolution of therapy-resistant cancer cells [37,130,131,135–141] and these processes are all highly relevant to cancer RT. Notably, further preclinical investigations revealed differences in the DNA repair proficiency between cells cultured under normal oxygen tensions compared to cells exposed to severely hypoxic conditions [54,55,142–145]. Furthermore, hypoxia is suspected to support certain aspects of tumor immune escape [146–149]. It is thus tempting to speculate that differences in DNA repair proficiency, the immune repertoire, or both might be exploited for a context-dependent radiosensitization of hypoxic tumors [150–154]. However, these innovative concepts will require extensive preclinical evaluation.

The progress in understanding the various molecular and cellular mechanisms underlying hypoxia-driven radiation resistance allowed for the development of innovative concepts for improving the RT response of solid tumors with substantial hypoxic fractions that warrant validation in independent preclinical studies and the clinical context.

Taken together, molecularly targeted drugs are expected to become part of future innovative RT and concurrent CRT protocols designed to treat solid tumors. Because of the broader availability of patient irradiation with photon beams so far, the *in vitro* and *in vivo* validation of such combinatorial approaches has been performed with photon irradiation. In the future, these biological approaches are likely to be combined with highly conformal RT and particle therapy, to harness the combined potential of all [155–157]. As mentioned above, successful clinical translation of such approaches will require the definition of reliable biomarkers or gene or protein expression signatures predictive for individual radiosensitivity of tumor and normal tissues and for responsiveness to specific therapies and diverse response modifiers [39,40,65–68,158]; such biomarkers for radiosensitivity profiles will help to individualize RT dose prescriptions and the selection of appropriate combination strategies in the future.

3. Current Preclinical Models to Assess Cellular Radiation Responses

Preclinical *in vitro* investigations in translational cancer research mostly focus on established cancer cell lines (2D, 3D, co-culture systems) as well as patient-derived primary cells, tissue slices (organotypic cultures), or organoid cultures derived from normal and cancer tissues, if available [158–165]. Organotypic tissue slice approaches offer the advantage to study effects in a more physiological cell–cell network context, retaining the native multicellularity, architecture, heterogeneity and physiology of the complex tumor-stroma interactions in the natural tumor microenvironment, at least in short-term cultures [166]. But the method requires access to patient samples, extensive experience and laborious optimization of culture conditions for extended culturing times [167], for avoiding tissue hypoxia, and for establishing appropriate clinically relevant end-points (for a comprehensive overview please refer to [168]). Once established, results with organotypic tissue slice cultures can be obtained within days suggesting that this method may be well suited for patient stratification in personalized medicine [168,169]. Though established from dissociated normal tissues or isolated cancer stem cells, organoids also comprise heterogeneous cell subtypes and their response to experimental treatments still more closely resembles the *in vivo* situation than cell lines. Besides, organoids with their cell–cell and cell-matrix interactions and the capacity of cellular differentiation offer a much higher complexity than traditional 2D cell systems [170]. However, the vascularization of a “natural” tumor and also its microenvironment influence cancer treatment responses and cannot easily be phenocopied neither by tissue slice cultures nor by organoids, although recent advances in organ-on-a-chip methods address this issue by connected chamber constructions mimicking, e.g., blood vasculature [171]. Besides, next to their genomic instability another major drawback of organoids is the limitation of available tissue entities (for review see: [172]). Moreover, current challenges of organoid research are on the one hand to increase organoid efficiency and to decrease the time for organoid outgrowth and on the other hand to lower the costs, and develop high-throughput screening [165].

The above *in vitro* models are complemented by classical xenograft or orthotopic murine tumor models with established human or syngeneic murine cancer cell lines, genetically engineered murine tumor models, or patient-derived xenograft tumors grown in immunodeficient mice [173–184].

So far, the “gold-standard” for the determination of cellular radiation sensitivity in radiobiology investigations has been the evaluation of clonogenic cell survival [37]. However, researchers in experimental radiation biology aim to develop alternative approaches [185] and at integrating improved models for designing their preclinical investigations as close as possible to the clinical situation, e.g., when performing mechanistic studies, to define therapeutic targets, or to evaluate novel combinatorial treatment strategies. However, each model system has its inherent advantages and disadvantages to answer specific research questions. Moreover, some of the above models require highly specialized knowledge, expensive specialized instrumentation, and/or access to patient material. These resources may only be available at larger cancer research centers or comprehensive cancer centers. The use of these model systems in translational cancer research as well as the inherent advantages and disadvantages have been recently reviewed elsewhere with a special focus on patient-derived organoid cultures, and will therefore not be discussed in detail here [170].

What has been neglected in many RT studies and cannot be addressed in almost all *in vitro* systems (except for tissue slice and organoid cultures), is that in addition to tumor cells, the tumor comprises also stroma cells, i.e., fibroblasts, endothelial cells, and cells of the immune system, embedded in tumor-specific extracellular matrix [186]. In recent years, it has become evident that stroma is not a passive scaffold-component of the tumor. Rather, stroma actively influences tumor growth and presents an important determinant of its responses to therapeutic interventions. Stroma regulates several aspects of tumor growth and maintenance, such the supply of oxygen and nutrients through the tumor vasculature, the signal input by growth factors and ECM molecules, and even the tumor-associated inflammation [187]. Vice-versa, tumor stroma is necessarily irradiated together with tumor cells and elicits local and systemic responses, likely to modify the overall tumor response, both locally and systemically [188–192]. The impact of vasculature [75,193–195], extracellular matrix [72,196,197], and

recruited immune cells [90,91,198,199] on RT response is actively debated and studied, and is thought to offer potential for innovation in the discovery of tumor radiosensitization targets. But further studies are required to enhance our understanding of the mechanisms regulating the interplay of tumor cells, stroma cells, ECM molecules, and recruited immune cells in tumor responses to RT.

4. The Chick Chorioallantoic Membrane (CAM) Assay

Between incubation day 4 and 10, the allantoic vesicle of the chick embryo enlarges and fuses with the adjacent mesodermal layer of the chorion to form the chorioallantoic membrane (CAM), which is highly vascularized and connected to the embryonic circulation by two arteries and one vein [200–203]. On gestation day 12, the CAM epithelium, physiologically serving as the chick embryo's lungs, surrounds the whole embryo (see Figure 1). Histologically, the CAM contains three major layers: (1) the ectoderm, which is attached to the shell membrane; (2) the mesoderm comprising a rich vascularization; and (3) the endoderm facing the allantoic cavity [204,205]. On gestation day 10, the CAM ectoderm capillary plexus connecting the arterial and venous blood vessels is fully developed. The vasculature not only plays an important role in chick embryo development, but using the CAM as a tumor model excessive vascularization also impacts inflammation and tumor growth. As a prerequisite for therapeutic intervention, a study by Soulet et al. mapped the molecular repertoire of the extracellular and membrane proteome associated with the vasculature and stroma [206]. In this context, most recently Mangir et al. reported on the use of the CAM assay to visualize tumor induced changes in vasculature [207].

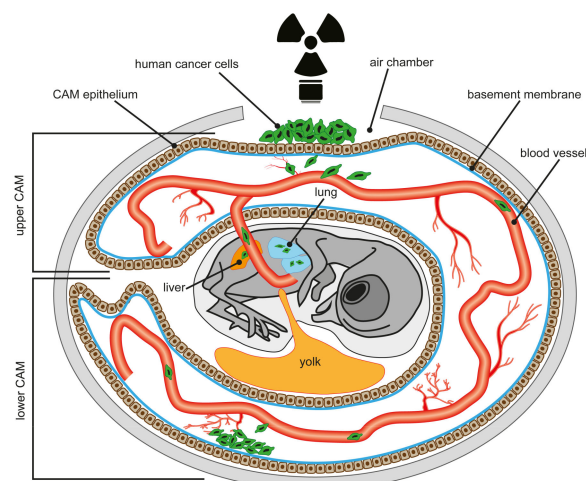


Figure 1. Schematic overview of the chorioallantoic membrane (CAM) assay. Modified after [201].

For CAM assays, fertilized eggs are incubated in a humidified rotary incubator at 38 °C and 50% humidity. Between embryonic (E) day 8, or preferentially E10, when the CAM vasculature is readily visible, the eggs are candled by shining light into the eggshell at the blunt end of the egg to locate the chorioallantoic vein, which is marked approximately 1 cm away from its branching point [208,209]. Afterwards, a hole is drilled through the blunt end of the egg into the air sac and the “upper CAM” is dropped by gentle suction, creating an artificial air chamber (see Figure 1). Another hole is drilled within the drawn square on the eggshell, the exposed CAM is gently abraded, e.g., by the use of a cotton-tipped applicator, and a suspension of cells or tissue biopsies can be placed onto the CAM. Then the window in the eggshell is sealed tightly with tape and the egg is returned to the incubator.

Already in 1958, human squamous cell carcinoma, sarcoma, adenocarcinoma, and bronchogenic carcinoma samples have been implanted onto the CAM, evaluated for the presence of metastases in the chick embryo and the efficiency chemotherapeutics on their growth [210]. Kaufman et al. (1956) were the firsts to describe changes in the CAM adjacent to the tumor inoculation site [211]. Dagg et al. (1956) used the CAM assay to investigate the metastasis of human squamous cell carcinoma, sarcoma,

and embryonal rhabdomyosarcoma on the CAM but also in the chick embryo [212]. Till then human tissue allo- and xenograft, e.g., from normal and cancerous bladder, liver, endometrium, adrenal gland, cerebellum, and skin have been successfully grafted onto the CAM by us and others and re-vascularize by developing anastomoses between donor and chick host vessels [213–215]. Besides, studies consolidated the CAM as a useful model to study metastasis [216,217].

The rapid development, tissue composition and the accessibility of the chick chorioallantoic membrane (CAM) for experimental manipulation provides an exceptionally useful preclinical *in vivo* model for scientists in different fields of research like bioengineering, biochemistry, transplant biology, cancer research, and drug development [218,219]. As the CAM is connected to the chick embryo by a rich vasculature network, this circulatory system is easily accessible for observations and manipulations. Besides, the CAM allows for real-time observations of treatment-induced changes in tumor cells *in vivo* [204]. Next to its well-known role as an angio- or anti-angiogenesis model (for review see: [200,202,220]), the CAM model reliably simulates key features of tumor growth in a few days and thus significantly speeds up research on human tumor progression and preclinical drug screening [219]. The CAM assay can be used for the evaluation of the activity and toxicity of a drug in the CAM as well as in grafted tumors or tumors forming from inoculated cells and also on the developing chick embryo itself, e.g., in terms of embryo death, inflammatory, and neo-vascularizing effects. A most recent review by DeBord et al. propagates the CAM as an increasingly valuable platform for patient-derived xenografts in preclinical oncology research [221]. As the CAM responds to injury with an inflammatory process similar to that in rabbit eye's conjunctival tissue, when it comes to testing for the irritancy potential of new chemicals, the CAM is likewise an *in vitro* alternative to the *in vivo* Draize rabbit eye test [222].

The nourishing vascularized structure of the CAM, enabling rapid tumor growth after inoculation of cells, also serves as an excellent metastasis model [205,208,209,223]. The capillary network of the CAM provides a repository for tumor cells disseminating from the primary site of grafting and intravasating into the hosts vasculature. For this purpose, fluorescent labeled, e.g., green-fluorescent protein (GFP)-labeled human cancer cells are inoculated on the upper CAM (see Figure 1). Depending on their tumorigenic potential the cells will eventually invade the upper CAM epithelium and basement membrane to enter a blood vessel. Highly aggressive cells thereby metastasize to the lower CAM, where they evade from the vasculature or invade the liver or lung of the chick embryo. Thus, in this setting the CAM provides an *in vivo* model to study the intravasation step of the metastatic cascade. The duration of the CAM assay is limited to a 7–9-day window available before the chick hatches. Tumors which form from the grafted cells are excised, measured, and photographed [223–225].

In the experimental migration setting, tumor cells are injected into a large CAM vein and the capillary system provides a site for initial arrest, but later on tumor cells may extravasate into the surrounding tissue [208,226]. After distinct time points standardized tissue punches of the lower CAM are collected, scanned for GFP-positive retinoblastoma RB cells by fluorescence microscopy, and collected in buffer or cryoconserved for RNA extraction. Intravasation, vascular dissemination, and migration of human tumor cells in the chick embryo's membranes and tissues can be quantified by flow cytometry analysis using a fluorescence-activated cell sorter (FACS), PCR mediated amplification of human-specific *Alu* sequences [208], or real-time PCR using human-specific primers, e.g., for glyceraldehyd-3-phosphat-dehydrogenase (GAPDH) [223,224,227].

On incubation day 3 or 4 the embryo and its extraembryonic membranes can also be transferred to a Petri dish and further incubated as an *ex ovo* culture [203,213,228]. This system improves the accessibility of the embryo and CAM tissue and facilitates live imaging and microsurgery applications [229,230]. Besides, this method allows for the analysis of several samples in one setting as well as the quantification of treatment responses over a larger CAM area. *Ex ovo* CAM experiments with chick embryos grown in a shell-less environment provide an ideal set up for high-resolution fluorescent microscopy approaches as the fluorescent-labeled chicken vasculature as well as labeled cancer cells can be visualized simultaneously; thus, all steps of the metastatic cancer cascade including cancer cell

migration and finally extravasation from the blood vessels can not only be imaged intravitally but also quantified using proper image analysis tools [231,232].

5. Advantages and Limitations of the CAM Assay

The CAM offers a plethora of advantages over the standard murine model to study, for example, therapy effects on tumor growth, the multistep process of tumor metastasis, angiogenesis, and drug sensitivity [233]. The CAM is naturally at least partially immune-deficient and thus, able to receive xenotransplants from various tissues and species without specific or nonspecific immune response. Another advantage is that the rich blood vessel and capillary vascular network of the CAM, naturally providing an interface for gas exchange for the chick embryo, also allows for survival, growth, and rapid vascularization of CAM tumors formed by inoculated cancer cells, but also bioptic patients' tissue specimens implanted on the CAM surface (for review see: [203–205,221,234–236]).

5.1. Biological Advantages

Compared to costly and time consuming rodent animal models, where tumor growth often takes up to 6 weeks, the CAM is an inexpensive, experimentally easily accessible, and quick model, in which tumors become visible between 2 and 5 days after tumor cell inoculation. Thus, the CAM allows for high-throughput screening of large sample numbers [203]. Another advantage of the CAM model is that cancer cells arrested in the CAM microcirculation survive and a large number extravasate while in standard rodent models intravenously injected tumor cells often rapidly perish before extravasation. Besides, labeled human tumor cells can not only be identified in the CAM, but also in the chick organs [237]. Strikingly, Chambers et al. described a higher number of tumors and metastases in a larger variety of organs after intravenous tumor cell injection in the chick vs. the murine model [217].

Although the duration of the CAM assay is limited to a time window before chick embryo hatching, CAM tumors developing from implanted cells or tissue biopsies have been successfully re-grafted by us [213] and others (for review see: [204,238,239]) prolonging the experimental time frame. Nonspecific inflammation, another limitation of the CAM model, can at least be partially prevented by an early onset of the implantation procedure (around day 9), when the chick's immune system is still completely immature.

5.2. Technical Advantages

Besides, while radiosensitizing experiments in mice require fixation of the animals under anesthesia, chick embryos can be easily irradiated without the need of any intricate operation [240].

5.3. Ethical Advantages

An ethical advantage of the CAM assay is that the CAM itself is not innervated and experiments are terminated before the development of centers in the brain associated with pain perception [203]. Thus, the chick embryo is not considered a living animal until E17 (in most countries) or even until hatching. At least in Germany the CAM assay is not classified as an animal experiment under the guidelines for handling laboratory animals, can be used without any ethical restriction and does not require protocol approval by an animal welfare or ethics committee. Table 1 provides a summarized overview of the main advantages of the CAM model compared to murine cancer models.

Table 1. Overview of advantages and limitations of the chick chorioallantoic membrane (CAM) model.

Issue	Studies in Mice	CAM Assay	Advantages CAM	Limitations CAM
Duration	4–9 (-12) weeks	3–5, max. 7 days	High throughput	Limited time frame for tumor growth and effects

Table 1. Cont.

Issue	Studies in Mice	CAM Assay	Advantages CAM	Limitations CAM
Experimental burden	Middle to high burden due to invasive treatment and tumor growth	No to low burden due to mainly extraembryonic tumor development	Meeting the 3R principle	
Costs	High expenses for breeding, keeping, feeding	Low expenses for eggs and transport	Cost-saving (approx. 60% saving of expenses)	
Space requirements	High; specific condition required	Low	Space-saving	
Permission requirements	Protocol approval by animal welfare and ethics committee	No approval by welfare or ethics committee required *	No administrative burden; quicker study start	
Functional analyses	Availability of antibodies, cytokines, primers			Limited number of avian-compatible antibodies, cytokines, primers

* applies for Germany.

6. The Immune System of the CAM

Tumors have been compared to a complex ecosystem as the cancer cells themselves are surrounded by a highly dynamic microenvironment consisting of extracellular matrix, and diverse cancer-associated cells, involved in the modulation of cancer cell activity and tumor progression [241,242]. While around a dozen successful patient-derived xenograft tissues of different tumor subtypes have been reported (for review see: [221]) and thus, the current literature strongly supports the CAM's potential as an efficient preclinical in vivo model, its use would highly benefit from a better understanding of the interaction of the CAM xenograft with the developing chick-host immune system. Inflammatory cells represent an important component of the tumor microenvironment. The production of T and B lymphocytes in the CAM starts around day 11, but immune cells are not fully mature before the chick embryo hatches at day 21 [243]. In day 10–15 chick embryos heterophils, the chick homolog of mammalian neutrophils, and monocytes are the two major inflammatory cell types present [205]. Klingenberg et al. described macrophages, lymphocytes, and heterophilic granulocytes to be the most abundant immune cells in CAM tumors formed from xenografted Burkitt lymphoma BL2B95 cells [244]. The authors propagate the applicability of the CAM model for research with a focus on tumor–stroma interaction [244]. A more recent study showing that MCF-7 breast cancer cells turn the CAM into a tumor stroma surrogate supports this notion [245].

7. Radiation Studies in and Ex Ovo

So far, only a limited number of research groups in the field of radiobiology make use of the CAM model to investigate the impact of ionizing radiation on tumor growth and therapy response as well as angiogenesis. Importantly, first reports reveal the successful implementation of the CAM as a preclinical xenograft tumor model to study different schedules of ionizing radiation and drug dose reduction options, providing leads for the optimization of combined CRT [246]. Along this line, Kauffmann et al. used the ex ovo CAM model to investigate the effects of 2.5–10 Gy irradiation on sliced patients' squamous cell carcinoma tumor specimen [229] as this system facilitates the access of tumor specimen not only for pharmaceutical applications but also for focused radiotherapy. Another study used the ex ovo chicken CAM to evaluate the effects of radiation combined with SPARC (secreted protein acidic and rich in cysteine) overexpression in neuroblastoma cells and describes a SPARC-induced reduction in radiation-induced angiogenesis [247]. More recently, another CAM study revealed a decrease in

colorectal carcinoma growth and radioresistance upon depletion of hnRNP K (heterogeneous nuclear ribonucleoprotein K) [248].

The CAM model has also been used as a bioassay to evaluate the potential of a variety of photosensitizers [249,250] and an *in vivo* model for photodynamic therapy or two-photon excitation [251,252] and is now propagated as an alternative to the mouse tumor model in the attempt to assay tumor response to photodynamic therapy [253].

The majority of research on the biological effects of ionizing radiation focused on its impact on DNA damage and cytotoxicity. Comparatively little is, however, known about radiation's effect on the microenvironment. For a long time, studies on the function of microenvironment on tumor progression have been hampered by the lack of an appropriate *in vivo* model till studies showed that the CAM is a highly suitable system for studying the interaction of tumors with the surrounding stroma [254,255].

When a tumor is subjected to radiotherapy, not only the cancer itself, but also the host cells are exposed to ionizing radiation. Macrophages, one major population of cells associated with tumors' innate immune response, have been shown to play an important role in tumor progression and modulating therapy response [256]. Since macrophages have been shown to induce angiogenesis via secreted pro-angiogenic cytokines and chemokines, Pinto et al. made use of the CAM assay to evaluate the angiogenic potential of conditioned medium from irradiated and non-irradiated macrophage-colorectal cancer co-cultures [256].

Growing tumors compensate for their constantly increasing oxygen consumption by angiogenesis and vasculogenesis. Thus, one major goal in fighting against cancer is the inhibition of angiogenesis. In this context, the effects of irradiation and a static magnetic field on tumor-induced angiogenesis was tested in CAM assays [257,258]. Moreover, a study by Brooks et al. demonstrated that at 20 cGy new blood vessel formation in the CAM is inhibited by 85%–90% [259]. Besides, the CAM model has been used to study the effects of X-rays—alone or in combination with substances like nitric oxide—on angiogenesis [260]. In 2001 Karnabatidis and colleagues evaluated the effect of ionizing radiation on the angiogenesis process in the CAM model [261]. A study on the effects of combining ionizing radiation with drug treatment did not reveal any anti-angiogenic effect of the drug, but further confirmed the notion that the CAM is a convenient model for radiobiological studies [262].

Thus, within a certain time window the CAM offers radiobiologist a real-time follow-up on RT and CRT induced changes in tumor size and (neo-)angiogenesis as well as early metastasis *in situ*, which can easily be documented by imaging. Besides, it serves an excellent model to study RT effects on tumor cell proliferation and apoptosis by excising CAM tumors developing from grafted tumor cells or patients' tumor biopsies after different radiation schedules or following different doses of CRT *ex vivo* and measuring cell viability, proliferation, and death via respective assays (e.g., WST-1, (TUNEL (terminal deoxynucleotidyl transferase dUTP nick end labeling assay), flow cytometry) in homogenates or immunohistochemically in histological sections. Moreover, radiation induced DNA damage and repair mechanisms and the effectiveness of radiosensitizing compounds suppressing DDR or DSB repair can be analyzed via PCR, electrophoresis, or immunohistochemically in samples from excised CAM tumors derived from inoculated tumor cells or tumor biopsies. A major advantage herein is the opportunity to perform such *in vivo* investigations in proton or heavy ion therapy centers that do not have opportunities for irradiation of small animals.

8. The CAM Model in Invasion Studies Under Hypoxia

The CAM model can also be used to study the effects of a hypoxic tumor microenvironment on tumor cell response to therapy, dissemination, and invasion. It has been shown that inoculated SW-490 colon carcinoma cells did not invade the epithelial layer of the CAM under normoxic conditions, but did under hypoxic conditions, indicating that hypoxia generates a more invasive phenotype of these tumor cells and establishing the CAM model for tumor invasion study under defined hypoxic conditions [263]. Along this line, Sun et al. employed the CAM invasion assays to show that hypoxia promotes ovarian cancer cell invasion via Snail-mediated upregulation of membrane-type

1 matrix metalloproteinase [264]. Another study used the CAM assay to characterize the effects of hypoxia-inducible factor-1 alpha (HIF-1), which is highly expressed under hypoxic conditions and commonly activated in tumors, especially in highly invasive and thus, aggressive tumors, on the angiogenic potential of small cell lung carcinoma cells [265]. In U87 glioma cell nodules, grafted on the CAM, the synthetic compound *myo*-inositol tri-pyrophosphate (ITPP), which increases the partial oxygen pressure (pO₂) in hypoxic tissues, markedly reduced tumor progression and angiogenesis [266].

A more recent study investigated the influence of hypoxia on disseminating human head and neck squamous cell carcinoma cell fate *in ovo*. In the study setting, a hypoxic microenvironment generated by a nano-intravital device (NANIVID) induced a subpopulation of dormant, post-hypoxic disseminating tumor cells, which evaded chemotherapy and might thus be the source of disease relapses [267].

Importantly, since tumor hypoxia is an important biologic constraint to the efficacy of radiotherapy, the CAM model may offer the opportunity to perform investigations about the effects of hypoxia on the radiotherapy response and combinatorial treatments to overcome hypoxia-induced radioresistance. In fact, Abe et al. demonstrated that adjunction of 8 Gy irradiation and application of 1 mg etanidazole, a hypoxic cell radiosensitizer, significantly decreases the size of CAM tumors forming after inoculation of EMT6/KU murine mammary cells [240].

9. Conclusions

Molecularly targeted drugs are expected to become part of future innovative complex CRT protocols including either photons or particle irradiation designed to treat solid tumors. On the basis of preclinical studies describing the CAM as a tumor stroma surrogate and propagating its applicability for experiments on tumor-stroma interaction and combinatorial treatments, we propose the CAM as a useful preclinical model for *in vivo* investigations of hypothesized synergistic effects of radiation–drug combinations. The implementation of the CAM assay in radiation research would allow for a time- and cost-limiting reduction of classical experimental animal models and for an ideal complementation of investigations with tumor organoids and organotypic tissue slice cultures, respectively. While CAM tumors developing from inoculated human cells are surrounded by chick tissue, organoids are only composed of one type of human cells, a fact that might prove advantageous for subsequent functional analyses. However, the embryonic microenvironment of the chick CAM provides the opportunity to additionally study its influence on tumor growth and metastatic progression. Another advantage of the CAM over organotypic tissue slice cultures and organoid models is that its rich capillary vascular network not only allows for growth, survival, and rapid vascularization of tumors developing from inoculated tumor cells without limitations, e.g., in oxygen availability of organotypic tissue slice cultures and of organoids, but also nourishes patient-derived xenografts, allowing for long-term growth and expansion. Furthermore, the blood vessel network of the CAM provides a repository for tumor cells disseminating from the primary site of grafting, thus allowing for fast invasion and metastasis studies. Besides, as developing and expanding CAM tumors are connected to the chick vasculature, on the one hand RT effects on vascular remodeling and (neo-)angiogenesis, on the other hand the impact of the vasculature on RT responses can be studied.

We assume that the CAM model may also be an ideal complementary preclinical *in vivo* model to study the relative biological effectiveness (RBE) of radiotherapy with photons compared to particle beams of different energies in clinically relevant tumor entities and to compare the radiosensitivity of xenografted normal and tumor tissues. Although the CAM assay proved to be an extremely useful supplementary tool for preclinical studies, thus possibly reducing animal studies, it will not be able to completely replace them as some limitations have to be taken into consideration. The duration of the CAM assay is limited to a maximum of 7 days, restricting the time for more complex studies involving sequential treatment or fractionated radiation schedules. Furthermore, the metabolism of drugs will probably not be reflected accurately in the CAM assay, potentially limiting its value as a preclinical assay in this respect. Finally, as the immune system of the developing chicken is not fully mature and

thus, does not resemble the adult human immune system, this aspect may limit application of the assay for immunotherapy-related studies. Nevertheless, the CAM assay will allow for high flexibility regarding the experimental design, e.g., screening of several molecularly targeted drugs, use of different radiation schedules and qualities, comparison of normal and tumor tissue responses, evaluation of the impact of hypoxia, and potential analyses of mechanisms regulating recruited immune cells in tumor response to RT including vascular immune effects. At the same time the CAM assay contributes to the ethical 3R (replacement, reduction, refinement) principle for the use of animals in research, although the presence of a developing chicken embryo may raise ethical issues as well.

Author Contributions: Conceptualization: N.D. and V.J.; writing – original draft preparation: N.D. and V.J.; writing- review and editing: N.D. and V.J.; visualization: N.D.; funding acquisition: N.D. and V.J.

Funding: This research was supported by grants of the Deutsche Forschungsgemeinschaft (DFG) grant number GRK1739/2, the German Cancer Aid (Deutsche Krebshilfe) grant number 70112711 (V.J.), the Bundesministerium für Bildung und Forschung (BMBF) grant number 02NUK47D (V.J.), the EU ITN RADIATE Council grant number 642623 (V.J.) and the Else-Kröner-Fresenius Stiftung foundation (N.D.)

Conflicts of Interest: The authors declare no conflict of interest.

References

- Bartelink, H.; Roelofsen, F.; Eschwege, F.; Rougier, P.; Bosset, J.F.; Gonzalez, D.G.; Peiffert, D.; van Glabbeke, M.; Pierart, M. Concomitant radiotherapy and chemotherapy is superior to radiotherapy alone in the treatment of locally advanced anal cancer: Results of a phase III randomized trial of the European Organization for Research and Treatment of Cancer Radiotherapy and Gastrointestinal Cooperative Groups. *JCO* **1997**, *15*, 2040–2049. [[CrossRef](#)]
- Yu, V.Y.; Nguyen, D.; Pajonk, F.; Kupelian, P.; Kaprealian, T.; Selch, M.; Low, D.A.; Sheng, K. Incorporating cancer stem cells in radiation therapy treatment response modeling and the implication in glioblastoma multiforme treatment resistance. *Int. J. Radiat. Oncol. Biol. Phys.* **2015**, *91*, 866–875. [[CrossRef](#)] [[PubMed](#)]
- Begg, A.C.; Stewart, F.A.; Vens, C. Strategies to improve radiotherapy with targeted drugs. *Nat. Rev. Cancer* **2011**, *11*, 239–253. [[CrossRef](#)] [[PubMed](#)]
- Herman, J.M.; Narang, A.K.; Griffith, K.A.; Zalupski, M.M.; Reese, J.B.; Gearhart, S.L.; Azad, N.S.; Chan, J.; Olsen, L.; Efron, J.E.; et al. The quality-of-life effects of neoadjuvant chemoradiation in locally advanced rectal cancer. *Int. J. Radiat. Oncol. Biol. Phys.* **2013**, *85*, e15–e19. [[CrossRef](#)]
- Morgan, M.A.; Parsels, L.A.; Maybaum, J.; Lawrence, T.S. Improving the efficacy of chemoradiation with targeted agents. *Cancer Discov.* **2014**, *4*, 280–291. [[CrossRef](#)]
- Budach, W.; Hehr, T.; Budach, V.; Belka, C.; Dietz, K. A meta-analysis of hyperfractionated and accelerated radiotherapy and combined chemotherapy and radiotherapy regimens in unresected locally advanced squamous cell carcinoma of the head and neck. *BMC Cancer* **2006**, *6*, 28. [[CrossRef](#)] [[PubMed](#)]
- De Ruysscher, D.; Niedermann, G.; Burnet, N.G.; Siva, S.; Lee, A.W.M.; Hegi-Johnson, F. Radiotherapy toxicity. *Nat. Rev. Dis. Primers* **2019**, *5*, 13. [[CrossRef](#)]
- Orth, M.; Lauber, K.; Niyazi, M.; Friedl, A.A.; Li, M.; Maihöfer, C.; Schüttrumpf, L.; Ernst, A.; Niemöller, O.M.; Belka, C. Current concepts in clinical radiation oncology. *Radiat. Environ. Biophys.* **2014**, *53*, 1–29. [[CrossRef](#)]
- Held, K.D.; Kawamura, H.; Kaminuma, T.; Paz, A.E.S.; Yoshida, Y.; Liu, Q.; Willers, H.; Takahashi, A. Effects of Charged Particles on Human Tumor Cells. *Front. Oncol.* **2016**, *6*, 23. [[CrossRef](#)]
- Schulz-Ertner, D.; Jäkel, O.; Schlegel, W. Radiation therapy with charged particles. *Semin. Radiat. Oncol.* **2006**, *16*, 249–259. [[CrossRef](#)]
- Paganetti, H.; van Luijk, P. Biological considerations when comparing proton therapy with photon therapy. *Semin. Radiat. Oncol.* **2013**, *23*, 77–87. [[CrossRef](#)] [[PubMed](#)]
- Plastaras, J.P.; Berman, A.T.; Freedman, G.M. Special cases for proton beam radiotherapy: Re-irradiation, lymphoma, and breast cancer. *Semin. Oncol.* **2014**, *41*, 807–819. [[CrossRef](#)] [[PubMed](#)]
- Suit, H.; DeLaney, T.; Goldberg, S.; Paganetti, H.; Clasie, B.; Gerweck, L.; Niemierko, A.; Hall, E.; Flanz, J.; Hallman, J.; et al. Proton vs carbon ion beams in the definitive radiation treatment of cancer patients. *Radiother. Oncol.* **2010**, *95*, 3–22. [[CrossRef](#)] [[PubMed](#)]

14. Schulz-Ertner, D.; Tsujii, H. Particle radiation therapy using proton and heavier ion beams. *J. Clin. Oncol.* **2007**, *25*, 953–964. [[CrossRef](#)] [[PubMed](#)]
15. Klein, C.; Dokic, I.; Mairani, A.; Mein, S.; Brons, S.; Häring, P.; Haberer, T.; Jäkel, O.; Zimmermann, A.; Zenke, F.; et al. Overcoming hypoxia-induced tumor radioresistance in non-small cell lung cancer by targeting DNA-dependent protein kinase in combination with carbon ion irradiation. *Radiat. Oncol.* **2017**, *12*, 208. [[CrossRef](#)] [[PubMed](#)]
16. Dai, Y.; Wei, Q.; Schwager, C.; Hanne, J.; Zhou, C.; Herfarth, K.; Rieken, S.; Lipson, K.E.; Debus, J.; Abdollahi, A. Oncogene addiction and radiation oncology: Effect of radiotherapy with photons and carbon ions in ALK-EML4 translocated NSCLC. *Radiat. Oncol.* **2018**, *13*, 1. [[CrossRef](#)]
17. Takahashi, W.; Nakajima, M.; Yamamoto, N.; Yamashita, H.; Nakagawa, K.; Miyamoto, T.; Tsuji, H.; Kamada, T.; Fujisawa, T. A prospective nonrandomized phase I/II study of carbon ion radiotherapy in a favorable subset of locally advanced non-small cell lung cancer (NSCLC). *Cancer* **2015**, *121*, 1321–1327. [[CrossRef](#)]
18. Zhou, C.; Moustafa, M.R.; Cao, L.; Kriegsmann, M.; Winter, M.; Schwager, C.; Jones, B.; Wang, S.; Bäuerle, T.; Zhou, P.-K.; et al. Modeling and multiscale characterization of the quantitative imaging based fibrosis index reveals pathophysiological, transcriptome and proteomic correlates of lung fibrosis induced by fractionated irradiation. *Int. J. Cancer* **2019**, *144*, 3160–3173. [[CrossRef](#)]
19. Zhou, C.; Jones, B.; Moustafa, M.; Yang, B.; Brons, S.; Cao, L.; Dai, Y.; Schwager, C.; Chen, M.; Jaekel, O.; et al. Determining RBE for development of lung fibrosis induced by fractionated irradiation with carbon ions utilizing fibrosis index and high-LET BED model. *Clin. Transl. Radiat. Oncol.* **2019**, *14*, 25–32. [[CrossRef](#)]
20. Graves, P.R.; Siddiqui, F.; Anscher, M.S.; Movsas, B. Radiation pulmonary toxicity: From mechanisms to management. *Semin. Radiat. Oncol.* **2010**, *20*, 201–207. [[CrossRef](#)]
21. Nishimura, H.; Miyamoto, T.; Yamamoto, N.; Koto, M.; Sugimura, K.; Tsujii, H. Radiographic pulmonary and pleural changes after carbon ion irradiation. *Int. J. Radiat. Oncol. Biol. Phys.* **2003**, *55*, 861–866. [[CrossRef](#)]
22. Hayashi, K.; Yamamoto, N.; Karube, M.; Nakajima, M.; Matsufuji, N.; Tsuji, H.; Ogawa, K.; Kamada, T. Prognostic analysis of radiation pneumonitis: Carbon-ion radiotherapy in patients with locally advanced lung cancer. *Radiat. Oncol.* **2017**, *12*, 91. [[CrossRef](#)] [[PubMed](#)]
23. Wu, Z.; Wang, X.; Yang, R.; Liu, Y.; Zhao, W.; Si, J.; Ma, X.; Sun, C.; Liu, Y.; Tan, Y.; et al. Effects of carbon ion beam irradiation on lung injury and pulmonary fibrosis in mice. *Exp. Ther. Med.* **2013**, *5*, 771–776. [[CrossRef](#)] [[PubMed](#)]
24. Sørensen, B.S.; Horsman, M.R.; Alsner, J.; Overgaard, J.; Durante, M.; Scholz, M.; Friedrich, T.; Bassler, N. Relative biological effectiveness of carbon ions for tumor control, acute skin damage and late radiation-induced fibrosis in a mouse model. *Acta Oncol.* **2015**, *54*, 1623–1630. [[CrossRef](#)] [[PubMed](#)]
25. Baumann, M.; Krause, M.; Overgaard, J.; Debus, J.; Bentzen, S.M.; Daartz, J.; Richter, C.; Zips, D.; Bortfeld, T. Radiation oncology in the era of precision medicine. *Nat. Rev. Cancer* **2016**, *16*, 234–249. [[CrossRef](#)]
26. Bolla, M.; de Reijke, T.M.; van Tienhoven, G.; van den Bergh, A.C.M.; Oodens, J.; Poortmans, P.M.P.; Gez, E.; Kil, P.; Akdas, A.; Soete, G.; et al. Duration of androgen suppression in the treatment of prostate cancer. *N. Engl. J. Med.* **2009**, *360*, 2516–2527. [[CrossRef](#)] [[PubMed](#)]
27. Bonner, J.A.; Harari, P.M.; Giralt, J.; Cohen, R.B.; Jones, C.U.; Sur, R.K.; Raben, D.; Baselga, J.; Spencer, S.A.; Zhu, J.; et al. Radiotherapy plus cetuximab for locoregionally advanced head and neck cancer: 5-year survival data from a phase 3 randomised trial, and relation between cetuximab-induced rash and survival. *Lancet Oncol.* **2010**, *11*, 21–28. [[CrossRef](#)]
28. D’Amico, A.V.; Manola, J.; Loffredo, M.; Renshaw, A.A.; DellaCroce, A.; Kantoff, P.W. 6-month androgen suppression plus radiation therapy vs radiation therapy alone for patients with clinically localized prostate cancer: A randomized controlled trial. *JAMA* **2004**, *292*, 821–827. [[CrossRef](#)]
29. Bentzen, J.; Toustrup, K.; Eriksen, J.G.; Primdahl, H.; Andersen, L.J.; Overgaard, J. Locally advanced head and neck cancer treated with accelerated radiotherapy, the hypoxic modifier nimorazole and weekly cisplatin. Results from the DAHANCA 18 phase II study. *Acta Oncol.* **2015**, *54*, 1001–1007. [[CrossRef](#)]
30. Formenti, S.C.; Demaria, S. Systemic effects of local radiotherapy. *Lancet Oncol.* **2009**, *10*, 718–726. [[CrossRef](#)]
31. Burnette, B.; Fu, Y.-X.; Weichselbaum, R.R. The confluence of radiotherapy and immunotherapy. *Front. Oncol.* **2012**, *2*. [[CrossRef](#)] [[PubMed](#)]

32. Chakravarti, A.; Wang, M.; Robins, H.I.; Lautenschlaeger, T.; Curran, W.J.; Brachman, D.G.; Schultz, C.J.; Choucair, A.; Dolled-Filhart, M.; Christiansen, J.; et al. RTOG 0211: A phase 1/2 study of radiation therapy with concurrent gefitinib for newly diagnosed glioblastoma patients. *Int. J. Radiat. Oncol. Biol. Phys.* **2013**, *85*, 1206–1211. [[CrossRef](#)] [[PubMed](#)]
33. Crane, C.H.; Winter, K.; Regine, W.F.; Safran, H.; Rich, T.A.; Curran, W.; Wolff, R.A.; Willett, C.G. Phase II study of bevacizumab with concurrent capecitabine and radiation followed by maintenance gemcitabine and bevacizumab for locally advanced pancreatic cancer: Radiation Therapy Oncology Group RTOG 0411. *J. Clin. Oncol.* **2009**, *27*, 4096–4102. [[CrossRef](#)] [[PubMed](#)]
34. Spigel, D.R.; Hainsworth, J.D.; Yardley, D.A.; Raefsky, E.; Patton, J.; Peacock, N.; Farley, C.; Burris, H.A.; Greco, F.A. Tracheoesophageal fistula formation in patients with lung cancer treated with chemoradiation and bevacizumab. *J. Clin. Oncol.* **2010**, *28*, 43–48. [[CrossRef](#)] [[PubMed](#)]
35. Rischin, D.; Peters, L.J.; O'Sullivan, B.; Giralt, J.; Fisher, R.; Yuen, K.; Trotti, A.; Bernier, J.; Bourhis, J.; Ringash, J.; et al. Tirapazamine, cisplatin, and radiation versus cisplatin and radiation for advanced squamous cell carcinoma of the head and neck (TROG 02.02, HeadSTART): A phase III trial of the Trans-Tasman Radiation Oncology Group. *J. Clin. Oncol.* **2010**, *28*, 2989–2995. [[CrossRef](#)] [[PubMed](#)]
36. Roos, W.P.; Kaina, B. DNA damage-induced cell death: From specific DNA lesions to the DNA damage response and apoptosis. *Cancer Lett.* **2013**, *332*, 237–248. [[CrossRef](#)]
37. Kirsch, D.G.; Diehn, M.; Kesarwala, A.H.; Maity, A.; Morgan, M.A.; Schwarz, J.K.; Bristow, R.; Demaria, S.; Eke, I.; Griffin, R.J.; et al. The Future of Radiobiology. *J. Natl. Cancer Inst.* **2018**, *110*, 329–340. [[CrossRef](#)]
38. Bristow, R.G.; Berlin, A.; Dal Pra, A. An arranged marriage for precision medicine: Hypoxia and genomic assays in localized prostate cancer radiotherapy. *Br. J. Radiol.* **2014**, *87*, 20130753. [[CrossRef](#)]
39. Scott, J.G.; Berglund, A.; Schell, M.J.; Mihaylov, I.; Fulp, W.J.; Yue, B.; Welsh, E.; Caudell, J.J.; Ahmed, K.; Strom, T.S.; et al. A genome-based model for adjusting radiotherapy dose (GARD): A retrospective, cohort-based study. *Lancet Oncol.* **2017**, *18*, 202–211. [[CrossRef](#)]
40. Bristow, R.G.; Alexander, B.; Baumann, M.; Bratman, S.V.; Brown, J.M.; Camphausen, K.; Choyke, P.; Citrin, D.; Contessa, J.N.; Dicker, A.; et al. Combining precision radiotherapy with molecular targeting and immunomodulatory agents: A guideline by the American Society for Radiation Oncology. *Lancet Oncol.* **2018**, *19*, e240–e251. [[CrossRef](#)]
41. Montay-Gruel, P.; Meziani, L.; Yakkala, C.; Vozenin, M.-C. Expanding the therapeutic index of radiation therapy by normal tissue protection. *Br. J. Radiol.* **2018**, 20180008. [[CrossRef](#)] [[PubMed](#)]
42. Jackson, S.P.; Bartek, J. The DNA-damage response in human biology and disease. *Nature* **2009**, *461*, 1071–1078. [[CrossRef](#)] [[PubMed](#)]
43. Helleday, T. Cancer phenotypic lethality, exemplified by the non-essential MTH1 enzyme being required for cancer survival. *Ann. Oncol.* **2014**, *25*, 1253–1255. [[CrossRef](#)] [[PubMed](#)]
44. Morgan, M.A.; Lawrence, T.S. Molecular Pathways: Overcoming Radiation Resistance by Targeting DNA Damage Response Pathways. *Clin. Cancer Res.* **2015**, *21*, 2898–2904. [[CrossRef](#)] [[PubMed](#)]
45. Lord, C.J.; Ashworth, A. The DNA damage response and cancer therapy. *Nature* **2012**, *481*, 287–294. [[CrossRef](#)]
46. Fokas, E.; Prevo, R.; Pollard, J.R.; Reaper, P.M.; Charlton, P.A.; Cornelissen, B.; Vallis, K.A.; Hammond, E.M.; Olcina, M.M.; Gillies McKenna, W.; et al. Targeting ATR in vivo using the novel inhibitor VE-822 results in selective sensitization of pancreatic tumors to radiation. *Cell Death Dis.* **2012**, *3*, e441. [[CrossRef](#)] [[PubMed](#)]
47. Biddlestone-Thorpe, L.; Sajjad, M.; Rosenberg, E.; Beckta, J.M.; Valerie, N.C.K.; Tokarz, M.; Adams, B.R.; Wagner, A.F.; Khalil, A.; Gilfor, D.; et al. ATM kinase inhibition preferentially sensitizes p53-mutant glioma to ionizing radiation. *Clin. Cancer Res.* **2013**, *19*, 3189–3200. [[CrossRef](#)]
48. Parsels, L.A.; Karnak, D.; Parsels, J.D.; Zhang, Q.; Vélez-Padilla, J.; Reichert, Z.R.; Wahl, D.R.; Maybaum, J.; O'Connor, M.J.; Lawrence, T.S.; et al. PARP1 Trapping and DNA Replication Stress Enhance Radiosensitization with Combined WEE1 and PARP Inhibitors. *Mol. Cancer Res.* **2018**, *16*, 222–232. [[CrossRef](#)]
49. Koniaras, K.; Cuddihy, A.R.; Christopoulos, H.; Hogg, A.; O'Connell, M.J. Inhibition of Chk1-dependent G2 DNA damage checkpoint radiosensitizes p53 mutant human cells. *Oncogene* **2001**, *20*, 7453–7463. [[CrossRef](#)]
50. Gad, H.; Koolmeister, T.; Jemth, A.-S.; Eshtad, S.; Jacques, S.A.; Ström, C.E.; Svensson, L.M.; Schultz, N.; Lundbäck, T.; Einarsdottir, B.O.; et al. MTH1 inhibition eradicates cancer by preventing sanitation of the dNTP pool. *Nature* **2014**, *508*, 215–221. [[CrossRef](#)]
51. Van Gent, D.C.; Kanaar, R. Exploiting DNA repair defects for novel cancer therapies. *Mol. Biol. Cell* **2016**, *27*, 2145–2148. [[CrossRef](#)] [[PubMed](#)]

52. Sanjiv, K.; Hagenkort, A.; Calderón-Montaño, J.M.; Koolmeister, T.; Reaper, P.M.; Mortusewicz, O.; Jacques, S.A.; Kuiper, R.V.; Schultz, N.; Scobie, M.; et al. Cancer-Specific Synthetic Lethality between ATR and CHK1 Kinase Activities. *Cell Rep.* **2016**, *14*, 298–309. [[CrossRef](#)] [[PubMed](#)]
53. Sulkowski, P.L.; Corso, C.D.; Robinson, N.D.; Scanlon, S.E.; Purshouse, K.R.; Bai, H.; Liu, Y.; Sundaram, R.K.; Hegan, D.C.; Fons, N.R.; et al. 2-Hydroxyglutarate produced by neomorphic IDH mutations suppresses homologous recombination and induces PARP inhibitor sensitivity. *Sci. Transl. Med.* **2017**, *9*. [[CrossRef](#)] [[PubMed](#)]
54. Chan, N.; Koritzinsky, M.; Zhao, H.; Bindra, R.; Glazer, P.M.; Powell, S.; Belmaaza, A.; Wouters, B.; Bristow, R.G. Chronic hypoxia decreases synthesis of homologous recombination proteins to offset chemoresistance and radioresistance. *Cancer Res.* **2008**, *68*, 605–614. [[CrossRef](#)] [[PubMed](#)]
55. Pires, I.M.; Bencokova, Z.; Milani, M.; Folkes, L.K.; Li, J.-L.; Stratford, M.R.; Harris, A.L.; Hammond, E.M. Effects of acute versus chronic hypoxia on DNA damage responses and genomic instability. *Cancer Res.* **2010**, *70*, 925–935. [[CrossRef](#)] [[PubMed](#)]
56. Stenerlöw, B.; Höglund, E.; Carlsson, J.; Blomquist, E. Rejoining of DNA fragments produced by radiations of different linear energy transfer. *Int. J. Radiat. Biol.* **2000**, *76*, 549–557. [[CrossRef](#)] [[PubMed](#)]
57. Jakob, B.; Scholz, M.; Taucher-Scholz, G. Biological imaging of heavy charged-particle tracks. *Radiat. Res.* **2003**, *159*, 676–684. [[CrossRef](#)]
58. Durante, M.; Loeffler, J.S. Charged particles in radiation oncology. *Nat. Rev. Clin. Oncol.* **2010**, *7*, 37–43. [[CrossRef](#)]
59. Sage, E.; Harrison, L. Clustered DNA lesion repair in eukaryotes: Relevance to mutagenesis and cell survival. *Mutat. Res.* **2011**, *711*, 123–133. [[CrossRef](#)]
60. Loucas, B.D.; Cornforth, M.N. The LET dependence of unrepaired chromosome damage in human cells: A break too far? *Radiat. Res.* **2013**, *179*, 393–405. [[CrossRef](#)]
61. Moore, S.; Stanley, F.K.T.; Goodarzi, A.A. The repair of environmentally relevant DNA double strand breaks caused by high linear energy transfer irradiation—no simple task. *DNA Repair (Amst)* **2014**, *17*, 64–73. [[CrossRef](#)] [[PubMed](#)]
62. Lorat, Y.; Brunner, C.U.; Schanz, S.; Jakob, B.; Taucher-Scholz, G.; Rube, C.E. Nanoscale analysis of clustered DNA damage after high-LET irradiation by quantitative electron microscopy—The heavy burden to repair. *DNA Repair (Amst)* **2015**, *28*, 93–106. [[CrossRef](#)] [[PubMed](#)]
63. Grosse, N.; Fontana, A.O.; Hug, E.B.; Lomax, A.; Coray, A.; Augsburg, M.; Paganetti, H.; Sartori, A.A.; Pruschy, M. Deficiency in homologous recombination renders Mammalian cells more sensitive to proton versus photon irradiation. *Int. J. Radiat. Oncol. Biol. Phys.* **2014**, *88*, 175–181. [[CrossRef](#)] [[PubMed](#)]
64. Oeck, S.; Szymonowicz, K.; Wiel, G.; Krysztofiak, A.; Lambert, J.; Koska, B.; Iliakis, G.; Timmermann, B.; Jendrossek, V. Relating Linear Energy Transfer to the Formation and Resolution of DNA Repair Foci After Irradiation with Equal Doses of X-ray Photons, Plateau, or Bragg-Peak Protons. *Int. J. Mol. Sci.* **2018**, *19*, 3779. [[CrossRef](#)] [[PubMed](#)]
65. Hess, J.; Unger, K.; Orth, M.; Schötz, U.; Schüttrumpf, L.; Zangen, V.; Gimenez-Aznar, I.; Michna, A.; Schneider, L.; Stamp, R.; et al. Genomic amplification of Fanconi anemia complementation group A (Fanca) in head and neck squamous cell carcinoma (HNSCC): Cellular mechanisms of radioresistance and clinical relevance. *Cancer Lett.* **2017**, *386*, 87–99. [[CrossRef](#)]
66. Michna, A.; Schötz, U.; Selmansberger, M.; Zitzelsberger, H.; Lauber, K.; Unger, K.; Hess, J. Transcriptomic analyses of the radiation response in head and neck squamous cell carcinoma subclones with different radiation sensitivity: Time-course gene expression profiles and gene association networks. *Radiat. Oncol.* **2016**, *11*, 94. [[CrossRef](#)]
67. Michna, A.; Braselmann, H.; Selmansberger, M.; Dietz, A.; Hess, J.; Gomolka, M.; Hornhardt, S.; Blüthgen, N.; Zitzelsberger, H.; Unger, K. Natural Cubic Spline Regression Modeling Followed by Dynamic Network Reconstruction for the Identification of Radiation-Sensitivity Gene Association Networks from Time-Course Transcriptome Data. *PLoS ONE* **2016**, *11*, e0160791. [[CrossRef](#)]
68. Jehmlich, N.; Stegmaier, P.; Golasowski, C.; Salazar, M.G.; Rischke, C.; Henke, M.; Völker, U. Differences in the whole saliva baseline proteome profile associated with development of oral mucositis in head and neck cancer patients undergoing radiotherapy. *J. Proteom.* **2015**, *125*, 98–103. [[CrossRef](#)]
69. Cheng, D.; Cao, N.; Chen, J.; Yu, X.; Shuai, X. Multifunctional nanocarrier mediated co-delivery of doxorubicin and siRNA for synergistic enhancement of glioma apoptosis in rat. *Biomaterials* **2012**, *33*, 1170–1179. [[CrossRef](#)]

70. Park, C.C.; Zhang, H.J.; Yao, E.S.; Park, C.J.; Bissell, M.J. Beta1 integrin inhibition dramatically enhances radiotherapy efficacy in human breast cancer xenografts. *Cancer Res.* **2008**, *68*, 4398–4405. [[CrossRef](#)]
71. Ahmed, K.M.; Zhang, H.; Park, C.C. NF- κ B regulates radioresistance mediated by β 1-integrin in three-dimensional culture of breast cancer cells. *Cancer Res.* **2013**, *73*, 3737–3748. [[CrossRef](#)] [[PubMed](#)]
72. Eke, I.; Zscheppang, K.; Dickreuter, E.; Hickmann, L.; Mazzeo, E.; Unger, K.; Krause, M.; Cordes, N. Simultaneous β 1 integrin-EGFR targeting and radiosensitization of human head and neck cancer. *J. Natl. Cancer Inst.* **2015**, *107*. [[CrossRef](#)] [[PubMed](#)]
73. Garcia-Barros, M.; Paris, F.; Cordon-Cardo, C.; Lyden, D.; Rafii, S.; Haimovitz-Friedman, A.; Fuks, Z.; Kolesnick, R. Tumor response to radiotherapy regulated by endothelial cell apoptosis. *Science* **2003**, *300*, 1155–1159. [[CrossRef](#)] [[PubMed](#)]
74. Potiron, V.A.; Abderrahmani, R.; Clément-Colmou, K.; Marionneau-Lambot, S.; Oullier, T.; Paris, F.; Supiot, S. Improved functionality of the vasculature during conventionally fractionated radiation therapy of prostate cancer. *PLoS ONE* **2013**, *8*, e84076. [[CrossRef](#)] [[PubMed](#)]
75. Klein, D. The Tumor Vascular Endothelium as Decision Maker in Cancer Therapy. *Front. Oncol.* **2018**, *8*, 367. [[CrossRef](#)] [[PubMed](#)]
76. Schaeue, D. A Century of Radiation Therapy and Adaptive Immunity. *Front. Immunol.* **2017**, *8*, 431. [[CrossRef](#)] [[PubMed](#)]
77. Brix, N.; Tiefenthaler, A.; Anders, H.; Belka, C.; Lauber, K. Abscopal, immunological effects of radiotherapy: Narrowing the gap between clinical and preclinical experiences. *Immunol. Rev.* **2017**, *280*, 249–279. [[CrossRef](#)]
78. Ganss, R.; Ryschich, E.; Klar, E.; Arnold, B.; Hämmerling, G.J. Combination of T-cell therapy and trigger of inflammation induces remodeling of the vasculature and tumor eradication. *Cancer Res.* **2002**, *62*, 1462–1470. [[PubMed](#)]
79. Dewan, M.Z.; Galloway, A.E.; Kawashima, N.; Dewyngaert, J.K.; Babb, J.S.; Formenti, S.C.; Demaria, S. Fractionated but not single-dose radiotherapy induces an immune-mediated abscopal effect when combined with anti-CTLA-4 antibody. *Clin. Cancer Res.* **2009**, *15*, 5379–5388. [[CrossRef](#)]
80. Lee, Y.; Auh, S.L.; Wang, Y.; Burnette, B.; Wang, Y.; Meng, Y.; Beckett, M.; Sharma, R.; Chin, R.; Tu, T.; et al. Therapeutic effects of ablative radiation on local tumor require CD8+ T cells: Changing strategies for cancer treatment. *Blood* **2009**, *114*, 589–595. [[CrossRef](#)]
81. Deng, L.; Liang, H.; Xu, M.; Yang, X.; Burnette, B.; Arina, A.; Li, X.-D.; Mauceri, H.; Beckett, M.; Darga, T.; et al. STING-Dependent Cytosolic DNA Sensing Promotes Radiation-Induced Type I Interferon-Dependent Antitumor Immunity in Immunogenic Tumors. *Immunity* **2014**, *41*, 843–852. [[CrossRef](#)] [[PubMed](#)]
82. Twyman-Saint Victor, C.; Rech, A.J.; Maity, A.; Rengan, R.; Pauken, K.E.; Stelekati, E.; Benci, J.L.; Xu, B.; Dada, H.; Odorizzi, P.M.; et al. Radiation and dual checkpoint blockade activate non-redundant immune mechanisms in cancer. *Nature* **2015**, *520*, 373–377. [[CrossRef](#)] [[PubMed](#)]
83. Rech, A.J.; Dada, H.; Kotzin, J.J.; Henao-Mejia, J.; Minn, A.J.; Twyman-Saint Victor, C.; Vonderheide, R.H. Radiotherapy and CD40 Activation Separately Augment Immunity to Checkpoint Blockade in Cancer. *Cancer Res.* **2018**, *78*, 4282–4291. [[CrossRef](#)] [[PubMed](#)]
84. Vanpouille-Box, C.; Alard, A.; Aryankalayil, M.J.; Sarfraz, Y.; Diamond, J.M.; Schneider, R.J.; Inghirami, G.; Coleman, C.N.; Formenti, S.C.; Demaria, S. DNA exonuclease Trex1 regulates radiotherapy-induced tumour immunogenicity. *Nat. Commun.* **2017**, *8*, 15618. [[CrossRef](#)] [[PubMed](#)]
85. Newton, J.M.; Hanoteau, A.; Liu, H.-C.; Gaspero, A.; Parikh, F.; Gartrell-Corrado, R.D.; Hart, T.D.; Laoui, D.; van Ginderachter, J.A.; Dharmaraj, N.; et al. Immune microenvironment modulation unmask therapeutic benefit of radiotherapy and checkpoint inhibition. *J. Immunother. Cancer* **2019**, *7*, 216. [[CrossRef](#)] [[PubMed](#)]
86. Herrera, F.G.; Bourhis, J.; Coukos, G. Radiotherapy combination opportunities leveraging immunity for the next oncology practice. *CA Cancer J. Clin.* **2017**, *67*, 65–85. [[CrossRef](#)] [[PubMed](#)]
87. Dar, T.B.; Henson, R.M.; Shiao, S.L. Targeting Innate Immunity to Enhance the Efficacy of Radiation Therapy. *Front. Immunol.* **2018**, *9*, 3077. [[CrossRef](#)] [[PubMed](#)]
88. Schulze, A.B.; Evers, G.; Kerkhoff, A.; Mohr, M.; Schliemann, C.; Berdel, W.E.; Schmidt, L.H. Future Options of Molecular-Targeted Therapy in Small Cell Lung Cancer. *Cancers (Basel)* **2019**, *11*, 690. [[CrossRef](#)]
89. Sevenich, L. Turning “Cold” Into “Hot” Tumors-Opportunities and Challenges for Radio-Immunotherapy Against Primary and Metastatic Brain Cancers. *Front. Oncol.* **2019**, *9*, 163. [[CrossRef](#)]
90. Formenti, S.C.; Demaria, S. Combining radiotherapy and cancer immunotherapy: A paradigm shift. *J. Natl. Cancer Inst.* **2013**, *105*, 256–265. [[CrossRef](#)]

91. Burnette, B.; Weichselbaum, R.R. Radiation as an immune modulator. *Semin. Radiat. Oncol.* **2013**, *23*, 273–280. [[CrossRef](#)] [[PubMed](#)]
92. Formenti, S.C.; Rudqvist, N.-P.; Golden, E.; Cooper, B.; Wennerberg, E.; Lhuillier, C.; Vanpouille-Box, C.; Friedman, K.; Ferrari de Andrade, L.; Wucherpennig, K.W.; et al. Radiotherapy induces responses of lung cancer to CTLA-4 blockade. *Nat. Med.* **2018**, *24*, 1845–1851. [[CrossRef](#)] [[PubMed](#)]
93. Vacchelli, E.; Bloy, N.; Aranda, F.; Buqué, A.; Cremer, I.; Demaria, S.; Eggermont, A.; Formenti, S.C.; Fridman, W.H.; Fucikova, J.; et al. Trial Watch: Immunotherapy plus radiation therapy for oncological indications. *Oncimmunology* **2016**, *5*, e1214790. [[CrossRef](#)] [[PubMed](#)]
94. Bernstein, M.B.; Krishnan, S.; Hodge, J.W.; Chang, J.Y. Immunotherapy and stereotactic ablative radiotherapy (ISABR): A curative approach? *Nat. Rev. Clin. Oncol.* **2016**, *13*, 516–524. [[CrossRef](#)] [[PubMed](#)]
95. Shaverdian, N.; Lisberg, A.E.; Bornazyan, K.; Veruttipong, D.; Goldman, J.W.; Formenti, S.C.; Garon, E.B.; Lee, P. Previous radiotherapy and the clinical activity and toxicity of pembrolizumab in the treatment of non-small-cell lung cancer: A secondary analysis of the KEYNOTE-001 phase 1 trial. *Lancet Oncol.* **2017**, *18*, 895–903. [[CrossRef](#)]
96. Antonia, S.J.; Villegas, A.; Daniel, D.; Vicente, D.; Murakami, S.; Hui, R.; Yokoi, T.; Chiappori, A.; Lee, K.H.; de Wit, M.; et al. Durvalumab after Chemoradiotherapy in Stage III Non-Small-Cell Lung Cancer. *N. Engl. J. Med.* **2017**, *377*, 1919–1929. [[CrossRef](#)] [[PubMed](#)]
97. Weichselbaum, R.R.; Liang, H.; Deng, L.; Fu, Y.-X. Radiotherapy and immunotherapy: A beneficial liaison? *Nat. Rev. Clin. Oncol.* **2017**, *14*, 365–379. [[CrossRef](#)] [[PubMed](#)]
98. Benci, J.L.; Xu, B.; Qiu, Y.; Wu, T.J.; Dada, H.; Twyman-Saint Victor, C.; Cucolo, L.; Lee, D.S.M.; Pauken, K.E.; Huang, A.C.; et al. Tumor Interferon Signaling Regulates a Multigenic Resistance Program to Immune Checkpoint Blockade. *Cell* **2016**, *167*, 1540–1554.e12. [[CrossRef](#)] [[PubMed](#)]
99. Wirsdörfer, F.; Jendrossek, V. Modeling DNA damage-induced pneumopathy in mice: Insight from danger signaling cascades. *Radiat. Oncol.* **2017**, *12*, 142. [[CrossRef](#)]
100. Arscott, W.T.; Zhu, S.; Plataras, J.P.; Maity, A.; Alonso-Basanta, M.; Jones, J. Acute neurologic toxicity of palliative radiotherapy for brain metastases in patients receiving immune checkpoint blockade. *Neurooncol. Pract.* **2019**, *6*, 297–304. [[CrossRef](#)]
101. Shibaki, R.; Akamatsu, H.; Fujimoto, M.; Koh, Y.; Yamamoto, N. Nivolumab induced radiation recall pneumonitis after two years of radiotherapy. *Ann. Oncol.* **2017**, *28*, 1404–1405. [[CrossRef](#)] [[PubMed](#)]
102. Wang, F.; Luo, Y.; Tian, X.; Ma, S.; Sun, Y.; You, C.; Gong, Y.; Xie, C. Impact of Radiotherapy Concurrent with Anti-PD-1 Therapy on the Lung Tissue of Tumor-Bearing Mice. *Radiat. Res.* **2019**, *191*, 271–277. [[CrossRef](#)] [[PubMed](#)]
103. Wennerberg, E.; Lhuillier, C.; Vanpouille-Box, C.; Pilonis, K.A.; García-Martínez, E.; Rudqvist, N.-P.; Formenti, S.C.; Demaria, S. Barriers to Radiation-Induced In Situ Tumor Vaccination. *Front. Immunol.* **2017**, *8*, 229. [[CrossRef](#)] [[PubMed](#)]
104. Wirsdörfer, F.; de Leve, S.; Jendrossek, V. Combining Radiotherapy and Immunotherapy in Lung Cancer: Can We Expect Limitations Due to Altered Normal Tissue Toxicity? *Int. J. Mol. Sci.* **2018**, *20*, 24. [[CrossRef](#)] [[PubMed](#)]
105. Brown, J.M.; Wilson, W.R. Exploiting tumour hypoxia in cancer treatment. *Nat. Rev. Cancer* **2004**, *4*, 437–447. [[CrossRef](#)] [[PubMed](#)]
106. Vaupel, P. Metabolic microenvironment of tumor cells: A key factor in malignant progression. *Exp. Oncol.* **2010**, *32*, 125–127. [[PubMed](#)]
107. Harris, A.L. Hypoxia—A key regulatory factor in tumour growth. *Nat. Rev. Cancer* **2002**, *2*, 38–47. [[CrossRef](#)]
108. Dewhirst, M.W.; Cao, Y.; Moeller, B. Cycling hypoxia and free radicals regulate angiogenesis and radiotherapy response. *Nat. Rev. Cancer* **2008**, *8*, 425–437. [[CrossRef](#)]
109. Horsman, M.R.; Mortensen, L.S.; Petersen, J.B.; Busk, M.; Overgaard, J. Imaging hypoxia to improve radiotherapy outcome. *Nat. Rev. Clin. Oncol.* **2012**, *9*, 674–687. [[CrossRef](#)]
110. Horsman, M.R.; Vaupel, P. Pathophysiological Basis for the Formation of the Tumor Microenvironment. *Front. Oncol.* **2016**, *6*, 66. [[CrossRef](#)]
111. Gray, L.H.; Conger, A.D.; Ebert, M.; Hornsey, S.; Scott, O.C. The concentration of oxygen dissolved in tissues at the time of irradiation as a factor in radiotherapy. *Br. J. Radiol.* **1953**, *26*, 638–648. [[CrossRef](#)]

112. Nordsmark, M.; Bentzen, S.M.; Rudat, V.; Brizel, D.; Lartigau, E.; Stadler, P.; Becker, A.; Adam, M.; Molls, M.; Dunst, J.; et al. Prognostic value of tumor oxygenation in 397 head and neck tumors after primary radiation therapy. An international multi-center study. *Radiother. Oncol.* **2005**, *77*, 18–24. [[CrossRef](#)] [[PubMed](#)]
113. Mortensen, L.S.; Johansen, J.; Kallehauge, J.; Primdahl, H.; Busk, M.; Lassen, P.; Alsner, J.; Sørensen, B.S.; Toustrup, K.; Jakobsen, S.; et al. FAZA PET/CT hypoxia imaging in patients with squamous cell carcinoma of the head and neck treated with radiotherapy: Results from the DAHANCA 24 trial. *Radiother. Oncol.* **2012**, *105*, 14–20. [[CrossRef](#)] [[PubMed](#)]
114. Horsman, M.R.; Overgaard, J. The impact of hypoxia and its modification of the outcome of radiotherapy. *J. Radiat. Res.* **2016**, *57* (Suppl. 1), i90–i98. [[CrossRef](#)]
115. Bristow, R.G.; Hill, R.P. Hypoxia and metabolism. Hypoxia, DNA repair and genetic instability. *Nat. Rev. Cancer* **2008**, *8*, 180–192. [[CrossRef](#)] [[PubMed](#)]
116. Liauw, S.L.; Connell, P.P.; Weichselbaum, R.R. New paradigms and future challenges in radiation oncology: An update of biological targets and technology. *Sci. Transl. Med.* **2013**, *5*, 173sr2. [[CrossRef](#)] [[PubMed](#)]
117. Vaupel, P.; Harrison, L. Tumor hypoxia: Causative factors, compensatory mechanisms, and cellular response. *Oncologist* **2004**, *9* (Suppl. 5), 4–9. [[CrossRef](#)]
118. Overgaard, J. Sensitization of hypoxic tumour cells—Clinical experience. *Int. J. Radiat. Biol.* **1989**, *56*, 801–811. [[CrossRef](#)]
119. Secomb, T.W.; Hsu, R.; Ong, E.T.; Gross, J.F.; Dewhirst, M.W. Analysis of the effects of oxygen supply and demand on hypoxic fraction in tumors. *Acta Oncol.* **1995**, *34*, 313–316. [[CrossRef](#)]
120. Secomb, T.W.; Hsu, R.; Braun, R.D.; Ross, J.R.; Gross, J.F.; Dewhirst, M.W. Theoretical simulation of oxygen transport to tumors by three-dimensional networks of microvessels. *Adv. Exp. Med. Biol.* **1998**, *454*, 629–634. [[CrossRef](#)]
121. Secomb, T.W.; Hsu, R.; Dewhirst, M.W. Synergistic effects of hyperoxic gas breathing and reduced oxygen consumption on tumor oxygenation: A theoretical model. *Int. J. Radiat. Oncol. Biol. Phys.* **2004**, *59*, 572–578. [[CrossRef](#)] [[PubMed](#)]
122. Ashton, T.M.; Fokas, E.; Kunz-Schughart, L.A.; Folkes, L.K.; Anbalagan, S.; Huether, M.; Kelly, C.J.; Pirovano, G.; Buffa, F.M.; Hammond, E.M.; et al. The anti-malarial atovaquone increases radiosensitivity by alleviating tumour hypoxia. *Nat. Commun.* **2016**, *7*, 12308. [[CrossRef](#)] [[PubMed](#)]
123. De Mey, S.; Jiang, H.; Corbet, C.; Wang, H.; Dufait, I.; Law, K.; Bastien, E.; Verovski, V.; Gevaert, T.; Feron, O.; et al. Antidiabetic Biguanides Radiosensitize Hypoxic Colorectal Cancer Cells Through a Decrease in Oxygen Consumption. *Front. Pharmacol.* **2018**, *9*, 1073. [[CrossRef](#)] [[PubMed](#)]
124. Benez, M.; Hong, X.; Vibhute, S.; Scott, S.; Wu, J.; Graves, E.; Le, Q.-T.; Koong, A.C.; Giaccia, A.J.; Yu, B.; et al. Papaverine and its derivatives radiosensitize solid tumors by inhibiting mitochondrial metabolism. *Proc. Natl. Acad. Sci. USA* **2018**, *115*, 10756–10761. [[CrossRef](#)] [[PubMed](#)]
125. Dewhirst, M.W. A potential solution for eliminating hypoxia as a cause for radioresistance. *Proc. Natl. Acad. Sci. USA* **2018**, *115*, 10548–10550. [[CrossRef](#)] [[PubMed](#)]
126. Bacon, A.L.; Harris, A.L. Hypoxia-inducible factors and hypoxic cell death in tumour physiology. *Ann. Med.* **2004**, *36*, 530–539. [[CrossRef](#)] [[PubMed](#)]
127. Comerford, K.M.; Wallace, T.J.; Karhausen, J.; Louis, N.A.; Montalto, M.C.; Colgan, S.P. Hypoxia-inducible factor-1-dependent regulation of the multidrug resistance (MDR1) gene. *Cancer Res.* **2002**, *62*, 3387–3394. [[PubMed](#)]
128. Liu, C.; Lin, Q.; Yun, Z. Cellular and molecular mechanisms underlying oxygen-dependent radiosensitivity. *Radiat. Res.* **2015**, *183*, 487–496. [[CrossRef](#)]
129. Wouters, B.G.; Koritzinsky, M. Hypoxia signalling through mTOR and the unfolded protein response in cancer. *Nat. Rev. Cancer* **2008**, *8*, 851–864. [[CrossRef](#)]
130. Span, P.N.; Bussink, J. Biology of hypoxia. *Semin. Nucl. Med.* **2015**, *45*, 101–109. [[CrossRef](#)]
131. Lee, C.-T.; Boss, M.-K.; Dewhirst, M.W. Imaging tumor hypoxia to advance radiation oncology. *Antioxid. Redox Signal.* **2014**, *21*, 313–337. [[CrossRef](#)] [[PubMed](#)]
132. Vaupel, P. Tumor microenvironmental physiology and its implications for radiation oncology. *Semin. Radiat. Oncol.* **2004**, *14*, 198–206. [[CrossRef](#)] [[PubMed](#)]
133. Ljungkvist, A.S.E.; Bussink, J.; Kaanders, J.H.A.M.; van der Kogel, A.J. Dynamics of tumor hypoxia measured with bioreductive hypoxic cell markers. *Radiat. Res.* **2007**, *167*, 127–145. [[CrossRef](#)] [[PubMed](#)]

134. Matsumoto, S.; Yasui, H.; Mitchell, J.B.; Krishna, M.C. Imaging cycling tumor hypoxia. *Cancer Res.* **2010**, *70*, 10019–10023. [[CrossRef](#)] [[PubMed](#)]
135. Tellier, C.; Desmet, D.; Petit, L.; Finet, L.; Graux, C.; Raes, M.; Feron, O.; Michiels, C. Cycling hypoxia induces a specific amplified inflammatory phenotype in endothelial cells and enhances tumor-promoting inflammation in vivo. *Neoplasia* **2015**, *17*, 66–78. [[CrossRef](#)] [[PubMed](#)]
136. Rankin, E.B.; Giaccia, A.J. Hypoxic control of metastasis. *Science* **2016**, *352*, 175–180. [[CrossRef](#)]
137. Dewhirst, M.W. Intermittent hypoxia furthers the rationale for hypoxia-inducible factor-1 targeting. *Cancer Res.* **2007**, *67*, 854–855. [[CrossRef](#)]
138. Hlouschek, J.; Ritter, V.; Wirsdörfer, F.; Klein, D.; Jendrossek, V.; Matschke, J. Targeting SLC25A10 alleviates improved antioxidant capacity and associated radioresistance of cancer cells induced by chronic-cycling hypoxia. *Cancer Lett.* **2018**, *439*, 24–38. [[CrossRef](#)]
139. Matschke, J.; Riffkin, H.; Klein, D.; Handrick, R.; Lüdemann, L.; Metzen, E.; Shlomi, T.; Stuschke, M.; Jendrossek, V. Targeted Inhibition of Glutamine-Dependent Glutathione Metabolism Overcomes Death Resistance Induced by Chronic Cycling Hypoxia. *Antioxid. Redox Signal.* **2016**, *25*, 89–107. [[CrossRef](#)]
140. Song, C.; Hong, B.-J.; Bok, S.; Lee, C.-J.; Kim, Y.-E.; Jeon, S.-R.; Wu, H.-G.; Lee, Y.-S.; Cheon, G.J.; Paeng, J.C.; et al. Real-time Tumor Oxygenation Changes After Single High-dose Radiation Therapy in Orthotopic and Subcutaneous Lung Cancer in Mice: Clinical Implication for Stereotactic Ablative Radiation Therapy Schedule Optimization. *Int. J. Radiat. Oncol. Biol. Phys.* **2016**, *95*, 1022–1031. [[CrossRef](#)]
141. Leung, E.; Cairns, R.A.; Chaudary, N.; Vellanki, R.N.; Kalliomaki, T.; Moriyama, E.H.; Mujcic, H.; Wilson, B.C.; Wouters, B.G.; Hill, R.; et al. Metabolic targeting of HIF-dependent glycolysis reduces lactate, increases oxygen consumption and enhances response to high-dose single-fraction radiotherapy in hypoxic solid tumors. *BMC Cancer* **2017**, *17*, 418. [[CrossRef](#)] [[PubMed](#)]
142. Meng, A.X.; Jalali, F.; Cuddihy, A.; Chan, N.; Bindra, R.S.; Glazer, P.M.; Bristow, R.G. Hypoxia down-regulates DNA double strand break repair gene expression in prostate cancer cells. *Radiother. Oncol.* **2005**, *76*, 168–176. [[CrossRef](#)] [[PubMed](#)]
143. Glazer, P.M.; Hegan, D.C.; Lu, Y.; Czochoch, J.; Scanlon, S.E. Hypoxia and DNA repair. *Yale J. Biol. Med.* **2013**, *86*, 443–451. [[PubMed](#)]
144. Rey, S.; Schito, L.; Koritzinsky, M.; Wouters, B.G. Molecular targeting of hypoxia in radiotherapy. *Adv. Drug Deliv. Rev.* **2017**, *109*, 45–62. [[CrossRef](#)] [[PubMed](#)]
145. Chan, N.; Ali, M.; McCallum, G.P.; Kumareswaran, R.; Koritzinsky, M.; Wouters, B.G.; Wells, P.G.; Gallinger, S.; Bristow, R.G. Hypoxia provokes base excision repair changes and a repair-deficient, mutator phenotype in colorectal cancer cells. *Mol. Cancer Res.* **2014**, *12*, 1407–1415. [[CrossRef](#)] [[PubMed](#)]
146. Sitkovsky, M.V.; Kjaergaard, J.; Lukashev, D.; Ohta, A. Hypoxia-adenosinergic immunosuppression: Tumor protection by T regulatory cells and cancerous tissue hypoxia. *Clin. Cancer Res.* **2008**, *14*, 5947–5952. [[CrossRef](#)]
147. Ohta, A. A Metabolic Immune Checkpoint: Adenosine in Tumor Microenvironment. *Front. Immunol.* **2016**, *7*, 109. [[CrossRef](#)]
148. Vaupel, P.; Multhoff, G. Hypoxia/HIF-1 α -Driven Factors of the Tumor Microenvironment Impeding Antitumor Immune Responses and Promoting Malignant Progression. *Adv. Exp. Med. Biol.* **2018**, *1072*, 171–175. [[CrossRef](#)]
149. Dewhirst, M.W.; Mowery, Y.M.; Mitchell, J.B.; Cherukuri, M.K.; Secomb, T.W. Rationale for hypoxia assessment and amelioration for precision therapy and immunotherapy studies. *J. Clin. Investing.* **2019**, *129*, 489–491. [[CrossRef](#)]
150. Chan, N.; Pires, I.M.; Bencokova, Z.; Coackley, C.; Luoto, K.R.; Bhogal, N.; Lakshman, M.; Gottipati, P.; Oliver, F.J.; Helleday, T.; et al. Contextual synthetic lethality of cancer cell kill based on the tumor microenvironment. *Cancer Res.* **2010**, *70*, 8045–8054. [[CrossRef](#)]
151. Olcina, M.; Lecane, P.S.; Hammond, E.M. Targeting hypoxic cells through the DNA damage response. *Clin. Cancer Res.* **2010**, *16*, 5624–5629. [[CrossRef](#)] [[PubMed](#)]
152. Sitkovsky, M.; Ohta, A. Targeting the hypoxia-adenosinergic signaling pathway to improve the adoptive immunotherapy of cancer. *J. Mol. Med.* **2013**, *91*, 147–155. [[CrossRef](#)] [[PubMed](#)]
153. McDonald, P.C.; Chafe, S.C.; Dedhar, S. Overcoming Hypoxia-Mediated Tumor Progression: Combinatorial Approaches Targeting pH Regulation, Angiogenesis and Immune Dysfunction. *Front. Cell Dev. Biol.* **2016**, *4*, 27. [[CrossRef](#)] [[PubMed](#)]

154. Hatfield, S.; Veszeleiova, K.; Steingold, J.; Sethuraman, J.; Sitkovsky, M. Mechanistic Justifications of Systemic Therapeutic Oxygenation of Tumors to Weaken the Hypoxia Inducible Factor 1 α -Mediated Immunosuppression. *Adv. Exp. Med. Biol.* **2019**, *1136*, 113–121. [[CrossRef](#)] [[PubMed](#)]
155. Helleday, T. Putting poly (ADP-ribose) polymerase and other DNA repair inhibitors into clinical practice. *Curr. Opin. Oncol.* **2013**, *25*, 609–614. [[CrossRef](#)] [[PubMed](#)]
156. Mitchell, J.; Smith, G.C.M.; Curtin, N.J. Poly(ADP-Ribose) polymerase-1 and DNA-dependent protein kinase have equivalent roles in double strand break repair following ionizing radiation. *Int. J. Radiat. Oncol. Biol. Phys.* **2009**, *75*, 1520–1527. [[CrossRef](#)] [[PubMed](#)]
157. Giaccia, A.J. Molecular Radiobiology: The State of the Art. *JCO* **2014**, *32*, 2871–2878. [[CrossRef](#)] [[PubMed](#)]
158. Eke, I.; Koch, U.; Hehlhans, S.; Sandfort, V.; Stanchi, F.; Zips, D.; Baumann, M.; Shevchenko, A.; Pilarsky, C.; Haase, M.; et al. PINCH1 regulates Akt1 activation and enhances radioresistance by inhibiting PP1 α . *J. Clin. Investing.* **2010**, *120*, 2516–2527. [[CrossRef](#)]
159. Nagle, P.W.; Hosper, N.A.; Barazzuol, L.; Jellema, A.L.; Baanstra, M.; van Goethem, M.-J.; Brandenburg, S.; Giesen, U.; Langendijk, J.A.; van Luijk, P.; et al. Lack of DNA Damage Response at Low Radiation Doses in Adult Stem Cells Contributes to Organ Dysfunction. *Clin. Cancer Res.* **2018**, *24*, 6583–6593. [[CrossRef](#)]
160. Bläuer, M.; Tammela, T.L.; Ylikomi, T. A novel tissue-slice culture model for non-malignant human prostate. *Cell Tissue Res.* **2008**, *332*, 489–498. [[CrossRef](#)]
161. Coppes, R.P.; Stokman, M.A. Stem cells and the repair of radiation-induced salivary gland damage. *Oral Dis.* **2011**, *17*, 143–153. [[CrossRef](#)] [[PubMed](#)]
162. Dijkstra, K.K.; Cattaneo, C.M.; Weeber, F.; Chalabi, M.; van de Haar, J.; Fanchi, L.F.; Slagter, M.; van der Velden, D.L.; Kaing, S.; Kelderman, S.; et al. Generation of Tumor-Reactive T Cells by Co-culture of Peripheral Blood Lymphocytes and Tumor Organoids. *Cell* **2018**, *174*, 1586–1598.e12. [[CrossRef](#)] [[PubMed](#)]
163. Sasaki, N.; Clevers, H. Studying cellular heterogeneity and drug sensitivity in colorectal cancer using organoid technology. *Curr. Opin. Genet. Dev.* **2018**, *52*, 117–122. [[CrossRef](#)] [[PubMed](#)]
164. Barkauskas, C.E.; Chung, M.-I.; Fioret, B.; Gao, X.; Katsura, H.; Hogan, B.L.M. Lung organoids: Current uses and future promise. *Development* **2017**, *144*, 986–997. [[CrossRef](#)] [[PubMed](#)]
165. Tuveson, D.; Clevers, H. Cancer modeling meets human organoid technology. *Science* **2019**, *364*, 952–955. [[CrossRef](#)] [[PubMed](#)]
166. Kocher, S.; Beyer, B.; Lange, T.; Nordquist, L.; Volquardsen, J.; Burdak-Rothkamm, S.; Schlomm, T.; Petersen, C.; Rothkamm, K.; Mansour, W.Y. A functional ex vivo assay to detect PARP1-EJ repair and radiosensitization by PARP-inhibitor in prostate cancer. *Int. J. Cancer* **2019**, *144*, 1685–1696. [[CrossRef](#)] [[PubMed](#)]
167. Naipal, K.A.T.; Verkaik, N.S.; Sánchez, H.; van Deurzen, C.H.M.; den Bakker, M.A.; Hoeijmakers, J.H.J.; Kanaar, R.; Vreeswijk, M.P.G.; Jager, A.; van Gent, D.C. Tumor slice culture system to assess drug response of primary breast cancer. *BMC Cancer* **2016**, *16*, 78. [[CrossRef](#)] [[PubMed](#)]
168. Meijer, T.G.; Naipal, K.A.; Jager, A.; van Gent, D.C. Ex vivo tumor culture systems for functional drug testing and therapy response prediction. *Future Sci. OA* **2017**, *3*, FSO190. [[CrossRef](#)]
169. Naipal, K.A.T.; Verkaik, N.S.; Ameziane, N.; van Deurzen, C.H.M.; Ter Brugge, P.; Meijers, M.; Sieuwerts, A.M.; Martens, J.W.; O'Connor, M.J.; Vrieling, H.; et al. Functional ex vivo assay to select homologous recombination-deficient breast tumors for PARP inhibitor treatment. *Clin. Cancer Res.* **2014**, *20*, 4816–4826. [[CrossRef](#)]
170. Nagle, P.W.; Plukker, J.T.M.; Muijs, C.T.; van Luijk, P.; Coppes, R.P. Patient-derived tumor organoids for prediction of cancer treatment response. *Semin. Cancer Biol.* **2018**, *53*, 258–264. [[CrossRef](#)]
171. Huh, D.; Hamilton, G.A.; Ingber, D.E. From 3D cell culture to organs-on-chips. *Trends Cell Biol.* **2011**, *21*, 745–754. [[CrossRef](#)]
172. Lancaster, M.A.; Huch, M. Disease modelling in human organoids. *Dis. Model. Mech.* **2019**, *12*. [[CrossRef](#)] [[PubMed](#)]
173. Marini, P.; Budach, W.; Niyazi, M.; Junginger, D.; Stickl, S.; Jendrossek, V.; Belka, C. Combination of the pro-apoptotic TRAIL-receptor antibody mapatumumab with ionizing radiation strongly increases long-term tumor control under ambient and hypoxic conditions. *Int. J. Radiat. Oncol. Biol. Phys.* **2009**, *75*, 198–202. [[CrossRef](#)] [[PubMed](#)]
174. Budach, W.; Budach, V.; Stuschke, M.; Dinges, S.; Sack, H. The TCD50 and regrowth delay assay in human tumor xenografts: Differences and implications. *Int. J. Radiat. Oncol. Biol. Phys.* **1993**, *25*, 259–268. [[CrossRef](#)]

175. Landgraf, M.; McGovern, J.A.; Friedl, P.; Huttmacher, D.W. Rational Design of Mouse Models for Cancer Research. *Trends Biotechnol.* **2018**, *36*, 242–251. [[CrossRef](#)] [[PubMed](#)]
176. Morton, J.J.; Bird, G.; Refaeli, Y.; Jimeno, A. Humanized Mouse Xenograft Models: Narrowing the Tumor-Microenvironment Gap. *Cancer Res.* **2016**, *76*, 6153–6158. [[CrossRef](#)] [[PubMed](#)]
177. Shultz, L.D.; Goodwin, N.; Ishikawa, F.; Hosur, V.; Lyons, B.L.; Greiner, D.L. Human cancer growth and therapy in immunodeficient mouse models. *Cold Spring Harb. Protoc.* **2014**, *2014*, 694–708. [[CrossRef](#)]
178. Byrne, A.T.; Alférez, D.G.; Amant, F.; Annibaldi, D.; Arribas, J.; Biankin, A.V.; Bruna, A.; Budinská, E.; Caldas, C.; Chang, D.K.; et al. Interrogating open issues in cancer medicine with patient-derived xenografts. *Nat. Rev. Cancer* **2017**, *17*, 632. [[CrossRef](#)]
179. Lai, Y.; Wei, X.; Lin, S.; Qin, L.; Cheng, L.; Li, P. Current status and perspectives of patient-derived xenograft models in cancer research. *J. Hematol. Oncol.* **2017**, *10*, 106. [[CrossRef](#)]
180. Willey, C.D.; Gilbert, A.N.; Anderson, J.C.; Gillespie, G.Y. Patient-Derived Xenografts as a Model System for Radiation Research. *Semin. Radiat. Oncol.* **2015**, *25*, 273–280. [[CrossRef](#)]
181. Khan, M.; Walters, L.L.; Li, Q.; Thomas, D.G.; Miller, J.M.L.; Zhang, Q.; Sciallis, A.P.; Liu, Y.; Dlouhy, B.J.; Fort, P.E.; et al. Characterization and pharmacologic targeting of EZH2, a fetal retinal protein and epigenetic regulator, in human retinoblastoma. *Lab. Investing.* **2015**, *95*, 1278–1290. [[CrossRef](#)] [[PubMed](#)]
182. Kahn, J.; Tofilon, P.J.; Camphausen, K. Preclinical models in radiation oncology. *Radiat. Oncol.* **2012**, *7*, 223. [[CrossRef](#)] [[PubMed](#)]
183. Koontz, B.F.; Verhaegen, F.; de Ruyscher, D. Tumour and normal tissue radiobiology in mouse models: How close are mice to mini-humans? *Br. J. Radiol.* **2017**, *90*, 20160441. [[CrossRef](#)] [[PubMed](#)]
184. Okada, S.; Vaeteewoottacharn, K.; Kariya, R. Application of Highly Immunocompromised Mice for the Establishment of Patient-Derived Xenograft (PDX) Models. *Cells* **2019**, *8*, 889. [[CrossRef](#)] [[PubMed](#)]
185. Unkel, S.; Belka, C.; Lauber, K. On the analysis of clonogenic survival data: Statistical alternatives to the linear-quadratic model. *Radiat. Oncol.* **2016**, *11*, 11. [[CrossRef](#)] [[PubMed](#)]
186. Hanahan, D.; Weinberg, R.A. Hallmarks of cancer: The next generation. *Cell* **2011**, *144*, 646–674. [[CrossRef](#)] [[PubMed](#)]
187. Barcellos-Hoff, M.H.; Lyden, D.; Wang, T.C. The evolution of the cancer niche during multistage carcinogenesis. *Nat. Rev. Cancer* **2013**, *13*, 511–518. [[CrossRef](#)]
188. Reisz, J.A.; Bansal, N.; Qian, J.; Zhao, W.; Furdui, C.M. Effects of ionizing radiation on biological molecules—Mechanisms of damage and emerging methods of detection. *Antioxid. Redox Signal.* **2014**, *21*, 260–292. [[CrossRef](#)]
189. Russell, J.S.; Brown, J.M. The irradiated tumor microenvironment: Role of tumor-associated macrophages in vascular recovery. *Front. Physiol.* **2013**, *4*, 157. [[CrossRef](#)]
190. Lauber, K.; Ernst, A.; Orth, M.; Herrmann, M.; Belka, C. Dying cell clearance and its impact on the outcome of tumor radiotherapy. *Front. Oncol.* **2012**, *2*, 116. [[CrossRef](#)]
191. Wirsdörfer, F.; Jendrossek, V. The Role of Lymphocytes in Radiotherapy-Induced Adverse Late Effects in the Lung. *Front. Immunol.* **2016**, *7*, 591. [[CrossRef](#)]
192. Schaeue, D.; Micewicz, E.D.; Ratikan, J.A.; Xie, M.W.; Cheng, G.; McBride, W.H. Radiation and inflammation. *Semin. Radiat. Oncol.* **2015**, *25*, 4–10. [[CrossRef](#)] [[PubMed](#)]
193. Moding, E.J.; Castle, K.D.; Perez, B.A.; Oh, P.; Min, H.D.; Norris, H.; Ma, Y.; Cardona, D.M.; Lee, C.-L.; Kirsch, D.G. Tumor cells, but not endothelial cells, mediate eradication of primary sarcomas by stereotactic body radiation therapy. *Sci. Transl. Med.* **2015**, *7*, 278ra34. [[CrossRef](#)] [[PubMed](#)]
194. Avraham, T.; Yan, A.; Zampell, J.C.; Daluvoy, S.V.; Haimovitz-Friedman, A.; Cordeiro, A.P.; Mehrara, B.J. Radiation therapy causes loss of dermal lymphatic vessels and interferes with lymphatic function by TGF-beta1-mediated tissue fibrosis. *Am. J. Physiol. Cell Physiol.* **2010**, *299*, C589–C605. [[CrossRef](#)] [[PubMed](#)]
195. Paris, F.; Fuks, Z.; Kang, A.; Capodiceci, P.; Juan, G.; Ehleiter, D.; Haimovitz-Friedman, A.; Cordon-Cardo, C.; Kolesnick, R. Endothelial apoptosis as the primary lesion initiating intestinal radiation damage in mice. *Science* **2001**, *293*, 293–297. [[CrossRef](#)] [[PubMed](#)]
196. Bai, C.; Yang, M.; Fan, Z.; Li, S.; Gao, T.; Fang, Z. Associations of chemo- and radio-resistant phenotypes with the gap junction, adhesion and extracellular matrix in a three-dimensional culture model of soft sarcoma. *J. Exp. Clin. Cancer Res.* **2015**, *34*, 58. [[CrossRef](#)] [[PubMed](#)]
197. Dickreuter, E.; Eke, I.; Krause, M.; Borgmann, K.; van Vugt, M.A.; Cordes, N. Targeting of $\beta 1$ integrins impairs DNA repair for radiosensitization of head and neck cancer cells. *Oncogene* **2016**, *35*, 1353–1362. [[CrossRef](#)]

198. Liang, H.; Deng, L.; Chmura, S.; Burnette, B.; Liadis, N.; Darga, T.; Beckett, M.A.; Lingen, M.W.; Witt, M.; Weichselbaum, R.R.; et al. Radiation-induced equilibrium is a balance between tumor cell proliferation and T cell-mediated killing. *J. Immunol.* **2013**, *190*, 5874–5881. [[CrossRef](#)]
199. Balermipas, P.; Rödel, F.; Liberz, R.; Oppermann, J.; Wagenblast, J.; Ghanaati, S.; Harter, P.N.; Mittelbronn, M.; Weiss, C.; Rödel, C.; et al. Head and neck cancer relapse after chemoradiotherapy correlates with CD163+ macrophages in primary tumour and CD11b+ myeloid cells in recurrences. *Br. J. Cancer* **2014**, *111*, 1509–1518. [[CrossRef](#)]
200. Ribatti, D. The Chick Embryo Chorioallantoic Membrane as an In Vivo Assay to Study Antiangiogenesis. *Pharmaceuticals (Basel)* **2010**, *3*, 482–513. [[CrossRef](#)]
201. Ribatti, D. The chick embryo chorioallantoic membrane as a model for tumor biology. *Exp. Cell Res.* **2014**, *328*, 314–324. [[CrossRef](#)]
202. Liu, M.; Xie, S.; Zhou, J. Use of animal models for the imaging and quantification of angiogenesis. *Exp. Anim.* **2018**, *67*, 1–6. [[CrossRef](#)]
203. Ribatti, D. The chick embryo chorioallantoic membrane (CAM). A multifaceted experimental model. *Mech. Dev.* **2016**, *141*, 70–77. [[CrossRef](#)]
204. Cimpean, A.M.; Ribatti, D.; Raica, M. The chick embryo chorioallantoic membrane as a model to study tumor metastasis. *Angiogenesis* **2008**, *11*, 311–319. [[CrossRef](#)] [[PubMed](#)]
205. Deryugina, E.I.; Quigley, J.P. Chapter 2. Chick Embryo Chorioallantoic Membrane Models to Quantify Angiogenesis Induced by Inflammatory and Tumor Cells or Purified Effector Molecules. *Methods Enzymol.* **2008**, *444*, 21–41. [[CrossRef](#)] [[PubMed](#)]
206. Soulet, F.; Kilarski, W.W.; Roux-Dalvai, F.; Herbert, M.J.; Sacewicz, I.; Mouton-Barbosa, E.; Bicknell, R.; Lalor, P.; Monsarrat, B.; Bikfalvi, A. Mapping the extracellular and membrane proteome associated with the vasculature and the stroma in the embryo. *Mol. Cell. Proteom.* **2013**, *12*, 2293–2312. [[CrossRef](#)] [[PubMed](#)]
207. Mangir, N.; Raza, A.; Haycock, J.W.; Chapple, C.; Macneil, S. An Improved In Vivo Methodology to Visualise Tumour Induced Changes in Vasculature Using the Chick Chorionic Allantoic Membrane Assay. *In Vivo* **2018**, *32*, 461–472. [[CrossRef](#)]
208. Zijlstra, A.; Mellor, R.; Panzarella, G.; Aimes, R.T.; Hooper, J.D.; Marchenko, N.D.; Quigley, J.P. A quantitative analysis of rate-limiting steps in the metastatic cascade using human-specific real-time polymerase chain reaction. *Cancer Res.* **2002**, *62*, 7083–7092.
209. Palmer, T.D.; Lewis, J.; Zijlstra, A. Quantitative analysis of cancer metastasis using an avian embryo model. *J. Vis. Exp.* **2011**. [[CrossRef](#)]
210. Harris, J.J. The human tumor grown in the egg. *Ann. N. Y. Acad. Sci.* **1958**, *76*, 764–769. [[CrossRef](#)]
211. Kaufman, N.; Kinney, T.D.; Mason, E.J.; Prieto, L.C. Maintenance of human neoplasm on the chick chorioallantoic membrane. *Am. J. Pathol.* **1956**, *32*, 271–285. [[PubMed](#)]
212. Dagg, C.P.; Karnofsky, D.A.; Roddy, J. Growth of transplantable human tumors in the chick embryo and hatched chick. *Cancer Res.* **1956**, *16*, 589–594. [[PubMed](#)]
213. Dohle, D.S.; Pasa, S.D.; Gustmann, S.; Laub, M.; Wissler, J.H.; Jennissen, H.P.; Dünker, N. Chick ex ovo culture and ex ovo CAM assay: How it really works. *J. Vis. Exp.* **2009**. [[CrossRef](#)] [[PubMed](#)]
214. Ausprunk, D.H.; Knighton, D.R.; Folkman, J. Vascularization of normal and neoplastic tissues grafted to the chick chorioallantois. Role of host and preexisting graft blood vessels. *Am. J. Pathol.* **1975**, *79*, 597–618. [[PubMed](#)]
215. Ausprunk, D.H.; Folkman, J. Vascular injury in transplanted tissues. Fine structural changes in tumor, adult, and embryonic blood vessels. *Virchows Arch. B Cell Pathol.* **1976**, *21*, 31–44.
216. Ossowski, L.; Reich, E. Experimental model for quantitative study of metastasis. *Cancer Res.* **1980**, *40*, 2300–2309. [[PubMed](#)]
217. Chambers, A.F.; Shafir, R.; Ling, V. A model system for studying metastasis using the embryonic chick. *Cancer Res.* **1982**, *42*, 4018–4025. [[PubMed](#)]
218. Nowak-Sliwinska, P.; Segura, T.; Iruela-Arispe, M.L. The chicken chorioallantoic membrane model in biology, medicine and bioengineering. *Angiogenesis* **2014**, *17*, 779–804. [[CrossRef](#)] [[PubMed](#)]
219. Swadi, R.; Mather, G.; Pizer, B.L.; Losty, P.D.; See, V.; Moss, D. Optimising the chick chorioallantoic membrane xenograft model of neuroblastoma for drug delivery. *BMC Cancer* **2018**, *18*. [[CrossRef](#)]

220. Nowak-Sliwinska, P.; Alitalo, K.; Allen, E.; Anisimov, A.; Aplin, A.C.; Auerbach, R.; Augustin, H.G.; Bates, D.O.; van Beijnum, J.R.; Bender, R.H.F.; et al. Consensus guidelines for the use and interpretation of angiogenesis assays. *Angiogenesis* **2018**, *21*, 425–532. [[CrossRef](#)] [[PubMed](#)]
221. DeBord, L.C.; Pathak, R.R.; Villaneuva, M.; Liu, H.-C.; Harrington, D.A.; Yu, W.; Lewis, M.T.; Sikora, A.G. The chick chorioallantoic membrane (CAM) as a versatile patient-derived xenograft (PDX) platform for precision medicine and preclinical research. *Am. J. Cancer Res.* **2018**, *8*, 1642–1660. [[PubMed](#)]
222. Palmeira-de-Oliveira, R.; Monteiro Machado, R.; Martinez-de-Oliveira, J.; Palmeira-de-Oliveira, A. Testing vaginal irritation with the Hen's Egg Test-Chorioallantoic Membrane assay. *ALTEX* **2018**, *35*, 495–503. [[CrossRef](#)] [[PubMed](#)]
223. Busch, M.; Philippeit, C.; Weise, A.; Dünker, N. Re-characterization of established human retinoblastoma cell lines. *Histochem. Cell Biol.* **2015**, *143*, 325–338. [[CrossRef](#)] [[PubMed](#)]
224. Busch, M.; Große-Kreul, J.; Wirtz, J.J.; Beier, M.; Stephan, H.; Royer-Pokora, B.; Metz, K.; Dünker, N. Reduction of the tumorigenic potential of human retinoblastoma cell lines by TFF1 overexpression involves p53/caspase signaling and miR-18a regulation. *Int. J. Cancer* **2017**, *141*, 549–560. [[CrossRef](#)] [[PubMed](#)]
225. Busch, M.; Papior, D.; Stephan, H.; Dünker, N. Characterization of etoposide- and cisplatin-chemoresistant retinoblastoma cell lines. *Oncol. Rep.* **2018**, *39*, 160–172. [[CrossRef](#)] [[PubMed](#)]
226. Kim, J.; Yu, W.; Kovalski, K.; Ossowski, L. Requirement for specific proteases in cancer cell intravasation as revealed by a novel semiquantitative PCR-based assay. *Cell* **1998**, *94*, 353–362. [[CrossRef](#)]
227. Große-Kreul, J.; Busch, M.; Winter, C.; Pikos, S.; Stephan, H.; Dünker, N. Forced Trefoil Factor Family Peptide 3 (TFF3) Expression Reduces Growth, Viability, and Tumorigenicity of Human Retinoblastoma Cell Lines. *PLoS ONE* **2016**, *11*, e0163025. [[CrossRef](#)]
228. Auerbach, R.; Kubai, L.; Knighton, D.; Folkman, J. A simple procedure for the long-term cultivation of chicken embryos. *Dev. Biol.* **1974**, *41*, 391–394. [[CrossRef](#)]
229. Kauffmann, P.; Troeltzsch, M.; Cordesmeier, R.; Heidekrueger, P.I.; Schliephake, H.; Canis, M.; Wolff, H.A.; Rave-Fraenk, M.; Stroebel, P.; Kehrer, A.; et al. Presentation of a variation of the chorioallantoic membrane set up as a potential model for individual therapy for squamous cell carcinoma of the oropharynx. *Clin. Hemorheol. Microcirc.* **2017**, *67*, 453–457. [[CrossRef](#)]
230. Farzaneh, M.; Attari, F.; Khoshnam, S.E.; Mozdziak, P.E. The method of chicken whole embryo culture using the eggshell windowing, surrogate eggshell and ex ovo culture system. *Br. Poult. Sci.* **2018**, *59*, 240–244. [[CrossRef](#)]
231. Willetts, L.; Bond, D.; Stoletov, K.; Lewis, J.D. Quantitative Analysis of Human Cancer Cell Extravasation Using Intravital Imaging. *Methods Mol. Biol.* **2016**, *1458*, 27–37. [[CrossRef](#)] [[PubMed](#)]
232. Leong, H.S.; Chambers, A.F.; Lewis, J.D. Assessing cancer cell migration and metastatic growth in vivo in the chick embryo using fluorescence intravital imaging. *Methods Mol. Biol.* **2012**, *872*, 1–14. [[CrossRef](#)] [[PubMed](#)]
233. Dupertuis, Y.M.; Delie, F.; Cohen, M.; Pichard, C. In ovo method for evaluating the effect of nutritional therapies on tumor development, growth and vascularization. *Clin. Nutr. Exp.* **2015**, *2*, 9–17. [[CrossRef](#)]
234. Ribatti, D. The chick embryo chorioallantoic membrane in the study of tumor angiogenesis. *Rom. J. Morphol. Embryol.* **2008**, *49*, 131–135. [[PubMed](#)]
235. Ribatti, D. Chapter 5. Chick Embryo Chorioallantoic Membrane as a Useful Tool to Study Angiogenesis. *Int. Rev. Cell. Mol. Biol.* **2008**, *270*, 181–224. [[CrossRef](#)] [[PubMed](#)]
236. Ribatti, D. The chick embryo chorioallantoic membrane (CAM) assay. *Reprod. Toxicol.* **2017**, *70*, 97–101. [[CrossRef](#)]
237. Bobek, V.; Plachy, J.; Pinterova, D.; Kolostova, K.; Boubelik, M.; Jiang, P.; Yang, M.; Hoffman, R.M. Development of a green fluorescent protein metastatic-cancer chick-embryo drug-screen model. *Clin. Exp. Metastasis* **2004**, *21*, 347–352. [[CrossRef](#)] [[PubMed](#)]
238. Murphy, J.B.; Rous, P. The Behavior of Chicken Sarcoma Implanted in the Developing Embryo. *J. Exp. Med.* **1912**, *15*, 119–132. [[CrossRef](#)]
239. Korngold, L.; Lipari, R. Tissue antigens of human tumors grown in rats, hamsters, and eggs. *Cancer Res.* **1955**, *15*, 159–161.
240. Abe, C.; Uto, Y.; Nakae, T.; Shinmoto, Y.; Sano, K.; Nakata, H.; Teraoka, M.; Endo, Y.; Maezawa, H.; Masunaga, S.-I.; et al. Evaluation of the in vivo Radiosensitizing Activity of Etanidazole Using Tumor-bearing Chick Embryo. *JRR* **2011**, *52*, 208–214. [[CrossRef](#)]

241. Joyce, J.A.; Pollard, J.W. Microenvironmental regulation of metastasis. *Nat. Rev. Cancer* **2009**, *9*, 239–252. [[CrossRef](#)] [[PubMed](#)]
242. Hanahan, D.; Coussens, L.M. Accessories to the crime: Functions of cells recruited to the tumor microenvironment. *Cancer Cell* **2012**, *21*, 309–322. [[CrossRef](#)] [[PubMed](#)]
243. Moreno-Jiménez, I.; Hulsart-Billstrom, G.; Lanham, S.A.; Janeczek, A.A.; Kontouli, N.; Kanczler, J.M.; Evans, N.D.; Oreffo, R.O. The chorioallantoic membrane (CAM) assay for the study of human bone regeneration: A refinement animal model for tissue engineering. *Sci. Rep.* **2016**, *6*, 32168. [[CrossRef](#)] [[PubMed](#)]
244. Klingenberg, M.; Becker, J.; Eberth, S.; Kube, D.; Wilting, J. The chick chorioallantoic membrane as an in vivo xenograft model for Burkitt lymphoma. *BMC Cancer* **2014**, *14*, 339. [[CrossRef](#)] [[PubMed](#)]
245. Comşa, Ş.; Popescu, R.; Avram, Ş.; Ceauşu, R.A.; Cîmpean, A.M.; Raica, M. Bevacizumab Modulation of the Interaction Between the MCF-7 Cell Line and the Chick Embryo Chorioallantoic Membrane. *In Vivo* **2017**, *31*, 199–203. [[CrossRef](#)] [[PubMed](#)]
246. Kleibeuker, E.A.; ten Hooven, M.A.; Castricum, K.C.; Honeywell, R.; Griffioen, A.W.; Verheul, H.M.; Slotman, B.J.; Thijssen, V.L. Optimal treatment scheduling of ionizing radiation and sunitinib improves the antitumor activity and allows dose reduction. *Cancer Med.* **2015**, *4*, 1003–1015. [[CrossRef](#)] [[PubMed](#)]
247. Boyineni, J.; Tanpure, S.; Gnanamony, M.; Antony, R.; Fernández, K.S.; Lin, J.; Pinson, D.; Gondi, C.S. SPARC overexpression combined with radiation retards angiogenesis by suppressing VEGF-A via miR-410 in human neuroblastoma cells. *Int. J. Oncol.* **2016**, *49*, 1394–1406. [[CrossRef](#)]
248. Eder, S.; Arndt, A.; Lamkowski, A.; Daskalaki, W.; Rump, A.; Priller, M.; Genze, F.; Wardelmann, E.; Port, M.; Steinestel, K. Baseline MAPK signaling activity confers intrinsic radioresistance to KRAS-mutant colorectal carcinoma cells by rapid upregulation of heterogeneous nuclear ribonucleoprotein K (hnRNP K). *Cancer Lett.* **2017**, *385*, 160–167. [[CrossRef](#)]
249. Hammer-Wilson, M.J.; Akian, L.; Espinoza, J.; Kimel, S.; Berns, M.W. Photodynamic parameters in the chick chorioallantoic membrane (CAM) bioassay for topically applied photosensitizers. *J. Photochem. Photobiol. B Biol.* **1999**, *53*, 44–52. [[CrossRef](#)]
250. Saw, C.L.L.; Olivo, M.; Chin, W.W.L.; Soo, K.C.; Heng, P.W.S. Transport of hypericin across chick chorioallantoic membrane and photodynamic therapy vasculature assessment. *Biol. Pharm. Bull.* **2005**, *28*, 1054–1060. [[CrossRef](#)]
251. Gottfried, V.; Lindenbaum, E.S.; Kimel, S. The chick chorioallantoic membrane (CAM) as an in vivo model for photodynamic therapy. *J. Photochem. Photobiol. B Biol.* **1992**, *12*, 204–207. [[CrossRef](#)]
252. Kimel, S.; Svaasand, L.O.; Hammer-Wilson, M.; Gottfried, V.; Cheng, S.; Svaasand, E.; Berns, M.W. Demonstration of synergistic effects of hyperthermia and photodynamic therapy using the chick chorioallantoic membrane model. *Lasers Surg. Med.* **1992**, *12*, 432–440. [[CrossRef](#)] [[PubMed](#)]
253. Honda, N.; Kariyama, Y.; Hazama, H.; Ishii, T.; Kitajima, Y.; Inoue, K.; Ishizuka, M.; Tanaka, T.; Awazu, K. Optical properties of tumor tissues grown on the chorioallantoic membrane of chicken eggs: Tumor model to assay of tumor response to photodynamic therapy. *J. Biomed. Opt.* **2015**, *20*, 125001. [[CrossRef](#)] [[PubMed](#)]
254. Becker, J.; Covelo-Fernandez, A.; von Bonin, F.; Kube, D.; Wilting, J. Specific tumor-stroma interactions of EBV-positive Burkitt's lymphoma cells in the chick chorioallantoic membrane. *Vasc. Cell* **2012**, *4*, 3. [[CrossRef](#)] [[PubMed](#)]
255. Fergelot, P.; Bernhard, J.-C.; Soulet, F.; Kilarski, W.W.; Léon, C.; Courtois, N.; Deminière, C.; Herbert, M.J.; Antczak, P.; Falciani, F.; et al. The experimental renal cell carcinoma model in the chick embryo. *Angiogenesis* **2013**, *16*, 181–194. [[CrossRef](#)] [[PubMed](#)]
256. Pinto, A.T.; Pinto, M.L.; Velho, S.; Pinto, M.T.; Cardoso, A.P.; Figueira, R.; Monteiro, A.; Marques, M.; Seruca, R.; Barbosa, M.A.; et al. Intricate Macrophage-Colorectal Cancer Cell Communication in Response to Radiation. *PLoS ONE* **2016**, *11*, e0160891. [[CrossRef](#)] [[PubMed](#)]
257. Ruggiero, M.; Bottaro, D.P.; Liguri, G.; Gulisano, M.; Peruzzi, B.; Pacini, S. 0.2 T magnetic field inhibits angiogenesis in chick embryo chorioallantoic membrane. *Bioelectromagnetics* **2004**, *25*, 390–396. [[CrossRef](#)]
258. Auerbach, R.; Arensman, R.; Kubai, L.; Folkman, J. Tumor-induced angiogenesis: Lack of inhibition by irradiation. *Int. J. Cancer* **1975**, *15*, 241–245. [[CrossRef](#)]
259. Brooks, P.C.; Roth, J.M.; Lymberis, S.C.; DeWyngaert, K.; Broek, D.; Formenti, S.C. Ionizing radiation modulates the exposure of the HUIV26 cryptic epitope within collagen type IV during angiogenesis. *Int. J. Radiat. Oncol. Biol. Phys.* **2002**, *54*, 1194–1201. [[CrossRef](#)]

260. Hatjikondi, O.; Ravazoula, P.; Kardamakis, D.; Dimopoulos, J.; Papaioannou, S. In vivo experimental evidence that the nitric oxide pathway is involved in the X-ray-induced antiangiogenicity. *Br. J. Cancer* **1996**, *74*, 1916–1923. [[CrossRef](#)]
261. Karnabatidis, D.; Dimopoulos, J.C.; Siablis, D.; Papazafiroopoulos, D.; Kalogeropoulou, C.P.; Nikiforidis, G. Quantification of the ionising radiation effect over angiogenesis in the chick embryo and its chorioallantoic membrane by computerised analysis of angiographic images. *Acta Radiol.* **2001**, *42*, 333–338. [[CrossRef](#)] [[PubMed](#)]
262. Kardamakis, D.; Hadjimichael, C.; Ginopoulos, P.; Papaioannou, S. Effects of paclitaxel in combination with ionizing radiation on angiogenesis in the chick embryo chorioallantoic membrane. A radiobiological study. *Strahlenther. Onkol.* **2004**, *180*, 152–156. [[CrossRef](#)] [[PubMed](#)]
263. Demir, R.; Naschberger, L.; Demir, I.; Melling, N.; Dimmler, A.; Papadopoulos, T.; Sturzl, M.; Klein, P.; Hohenberger, W. Hypoxia generates a more invasive phenotype of tumour cells: An in vivo experimental setup based on the chorioallantoic membrane. *Pathol. Oncol. Res.* **2009**, *15*, 417–422. [[CrossRef](#)] [[PubMed](#)]
264. Sun, L.; Lin, P.; Qin, Z.; Liu, Y.; Deng, L.-L.; Lu, C. Hypoxia promotes HO-8910PM ovarian cancer cell invasion via Snail-mediated MT1-MMP upregulation. *Exp. Biol. Med. (Maywood)* **2015**, *240*, 1434–1445. [[CrossRef](#)] [[PubMed](#)]
265. Wan, J.; Chai, H.; Yu, Z.; Ge, W.; Kang, N.; Xia, W.; Che, Y. HIF-1 α effects on angiogenic potential in human small cell lung carcinoma. *J. Exp. Clin. Cancer Res.* **2011**, *30*, 77. [[CrossRef](#)] [[PubMed](#)]
266. Sihn, G.; Walter, T.; Klein, J.-C.; Queguiner, I.; Iwao, H.; Nicolau, C.; Lehn, J.-M.; Corvol, P.; Gasc, J.-M. Anti-angiogenic properties of myo-inositol trispyrophosphate in ovo and growth reduction of implanted glioma. *FEBS Lett.* **2007**, *581*, 962–966. [[CrossRef](#)] [[PubMed](#)]
267. Fluegen, G.; Avivar-Valderas, A.; Wang, Y.; Padgen, M.R.; Williams, J.K.; Nobre, A.R.; Calvo, V.; Cheung, J.F.; Bravo-Cordero, J.J.; Entenberg, D.; et al. Phenotypic heterogeneity of disseminated tumour cells is preset by primary tumour hypoxic microenvironments. *Nat. Cell Biol.* **2017**, *19*, 120–132. [[CrossRef](#)] [[PubMed](#)]



© 2019 by the authors. Licensee MDPI, Basel, Switzerland. This article is an open access article distributed under the terms and conditions of the Creative Commons Attribution (CC BY) license (<http://creativecommons.org/licenses/by/4.0/>).